Linea - Progetti Speciali

RS2 - Simulazioni di terremoti ed effetti near-source

COORDINATORE: Roberto Paolucci – Politecnico di Milano

Gruppo di lavoro UNIPV: Carlo G. Lai, PhD
Elisa Zuccolo, PhD

Riunione di kick-off, Napoli, 27-03-2014

SOMMARIO

- **ReLuis 2: Obiettivi realizzati**
- **ReLuis 3: Attività pianificate per il primo anno**

ReLuis 2: Obiettivi realizzati

Definizione di spettri di risposta elastici di normativa tenendo conto degli effetti di campo-vicino

<u>Linea Trasversale geotecnica</u>

Macrotema MT1 – Analisi di risposta sismica locale e lifelines

Coordinatore: Francesco Silvestri - Università di Napoli ‘Federico II’

Task *MT1.3: <u>Problemi near-fault ed effetti delle discontinuità nel sottosuolo sulla RSL</u>*

Overview of existing seismic codes worldwide that take into account near-fault effects in defining the seismic input

Norms that include near fault effects in defining seismic input:

- *UBC-Uniform Building Code (1997)*
- *Seismic Design Code for Buildings in Taiwan (2005)*
- *New Zealand Standard (2004)*
- *IBC-International Building Code (2006; 2009)*

UBC (1997)

Two "*near-fault*" factors N_a (short period) and N_v (long period)
N_a, N_v=f(D,fault type) for seismic zone 4

Table 1. Near source factor N_a (from Table 16-S from UBC-97).

	Closest distance to known seismic source		
Seismic source type	**≤ 2km**	**5km**	**≥ 10km**
A	1.5	1.2	1.0
B	1.3	1.0	1.0
C	1.0	1.0	1.0

Table 2. Near source factor N_v (from Table 16-T from UBC-97).

	Closest distance to known seismic source			
Seismic source type	**≤ 2km**	**5km**	**10km**	**≥ 15km**
A	2.0	1.6	1.2	1.0
B	1.6	1.2	1.0	1.0
C	1.0	1.0	1.0	1.0

Table 3. Seismic source type (from Table 16-U of UBC-97).

		Seismic source definition	
Seismic Source Type	**Seismic Source Description**	**Maximum M_w**	**Slip Rate, SR (mm/year)**
A	Faults that are capable of producing large magnitude events and that have a high rate of seismic activity	M ≥ 7.0	SR ≥ 5
B	All faults other than Types A and C	M ≥ 7.0	SR < 5
		M < 7.0	SR > 2
		M ≥ 6.5	SR < 2
C	Faults that are not capable of producing large magnitude earthquakes and that have a relatively low rate of seismic activity	M < 6.5	SR ≤ 2

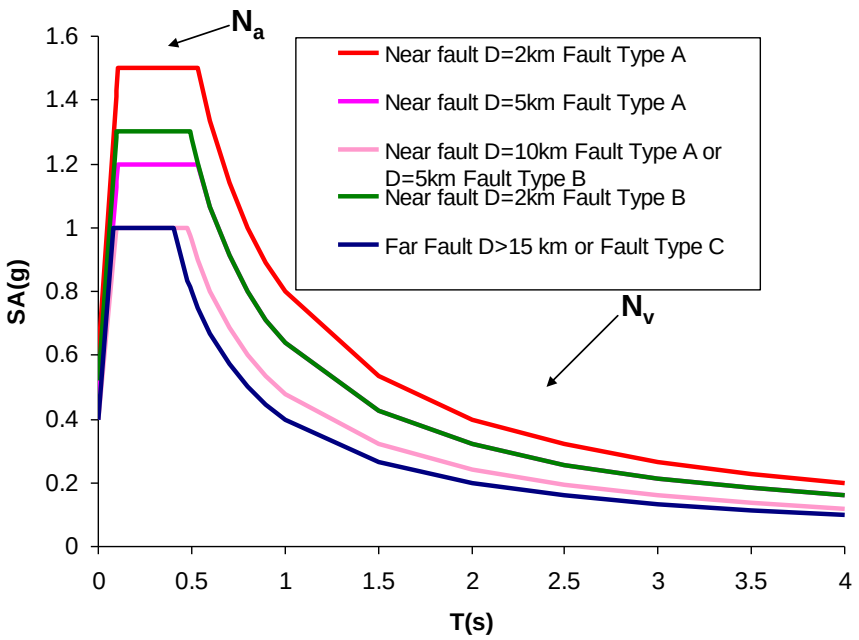

Seismic Design Code for Buildings in Taiwan (2005)

Two "*near-fault*" factors N_a (short period) and N_v (long period) defined for several active faults in Taiwan

Table 8. Near-fault factors for Chelungpu fault (from Jan *et al.*, 2010).

	r ≤ 2km	2km < r ≤ 5km	5km < r ≤ 8km	8km < r ≤ 12km
N_A	1.23	1.16	1.07	1.03
N_V	1.36	1.32	1.22	1.10

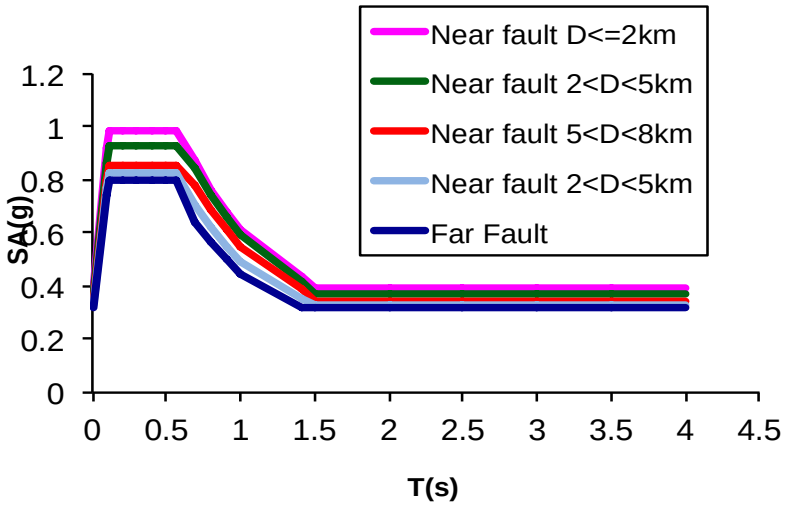

New Zealand Standard (2004)

One near-fault factor N(T,D) for T≥1.5 s

3.1.6.1 *Annual probability of exceedance* $\geq 1/250$

$$N(T,D) = 1.0$$

3.1.6.2 *Annual probability of exceedance* $< 1/250$

$$N(T,D) = N_{max}(T) \qquad D \leq 2 \text{ km}$$

$$= 1 + (N_{max}(T) - 1)\ \frac{20 - D}{18} \qquad 2 \text{ km} < D \leq 20 \text{ km}$$

$$= 1.0 \qquad D > 20 \text{ km}$$

Soil type A, RT=500 years

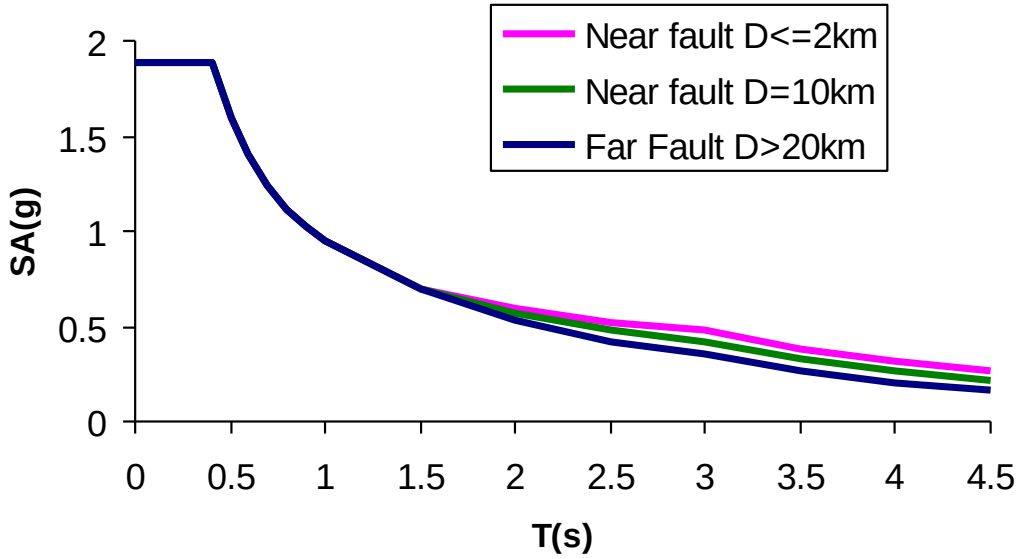

MAXIMUM NEAR-FAULT FACTORS $N_{max}(T)$

Period T s	$N_{max}(T)$
≤ 1.5	1.0
2	1.12
3	1.36
4	1.60
≥ 5	1.72

#	Location	Z	D(km)[1]
91	Greymouth	0.37	-
92	Kaikoura	0.42	12
93	Harihari	0.46	4
94	Hokitika	0.45	-
95	Fox Glacier	0.44	≤ 2
96	Franz Josef	0.44	≤ 2
97	Otira	0.60	3
98	Arthurs Pass	0.60	12
99	Rangiora	0.33	-
100	Darfield	0.30	-

IBC-International Building Code (2006; 2009)

11.4.7 Site-Specific Ground Motion Procedures

The site-specific ground motion procedures set forth in Chapter 21 are permitted to be used to determine ground motions for any structure. A site response analysis shall be performed in accordance with Section 21.1 for structures on Site Class F sites, unless the exception to Section 20.3.1 is applicable. For seismically isolated structures and for structures with damping systems on sites with S_1 greater than or equal to 0.6, a ground motion hazard analysis shall be performed in accordance with Section 21.2.

21.2 RISK-TARGETED MAXIMUM CONSIDERED EARTHQUAKE (MCE_R) GROUND MOTION HAZARD ANALYSIS

or required by Section 11.4.7. The ground motion hazard analysis shall account for the regional tectonic setting, geology, and seismicity, the expected recurrence rates and maximum magnitudes of earthquakes on known faults and source zones, the characteristics of ground motion attenuation, near source effects, if any, on ground motions, and the effects of subsurface site conditions on ground motions. The characteristics

21.2.3 Site-Specific MCE_R

The site-specific MCE_R spectral response acceleration at any period, S_{aM}, shall be taken as the lesser of the spectral response accelerations from the probabilistic ground motions of Section 21.2.1 and the deterministic ground motions of Section 21.2.2.

near-fault effects directly evaluated by either probabilistic and/or deterministic seismic hazard analyses

UBC-Uniform Building Code (1997)

Seismic Design Code for Buildings in Taiwan (2005)

New Zealand Standard (2004)

IBC-International Building Code (2006; 2009)

consider the near fault effect as a **broad-band effect** with amplitudes increasing with magnitude (Somerville et al., 1997) and decreasing with distance from the fault

BUT

the near fault effect is **narrow band**, with a peak corresponding to a dominant period which increases with magnitude Tp=f(M,soil type) (Somerville, 2003)

Characteristics of near-fault motion

M_w7.3 1992 Landers Earthquake

Near-fault pulse

Short duration
Large amplitude

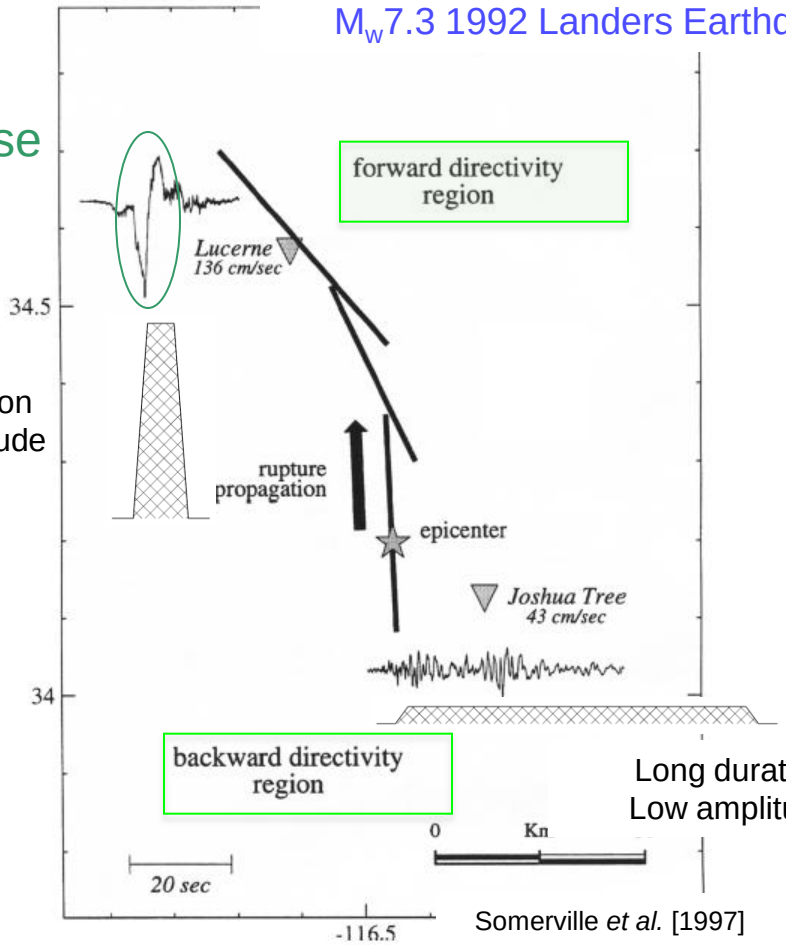

Long duration
Low amplitude

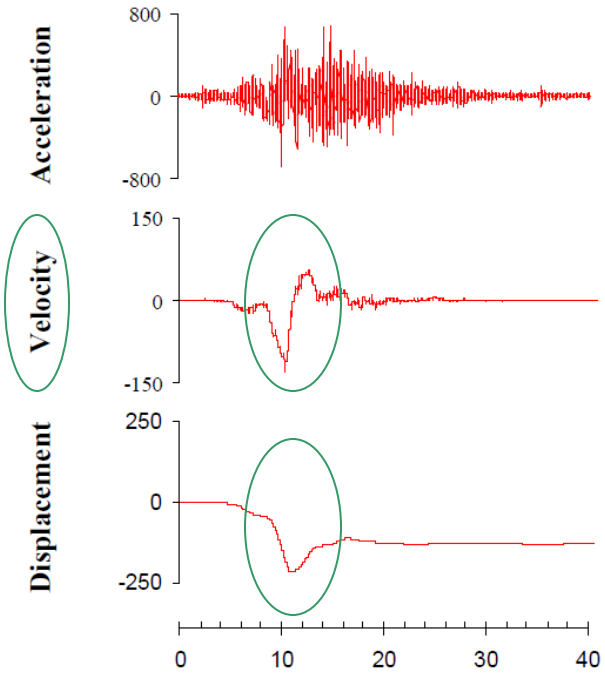

Somerville *et al.* [1997]

Response spectra

The elastic response spectra have peaks that are related to the period of the pulse. Somerville (2003): the velocity response spectra tend to have a peak at about 0.85 times the period of the pulse.

Simple time-domain pulses

Somerville [2003]

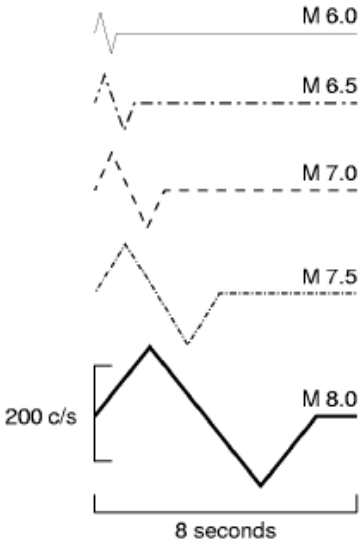

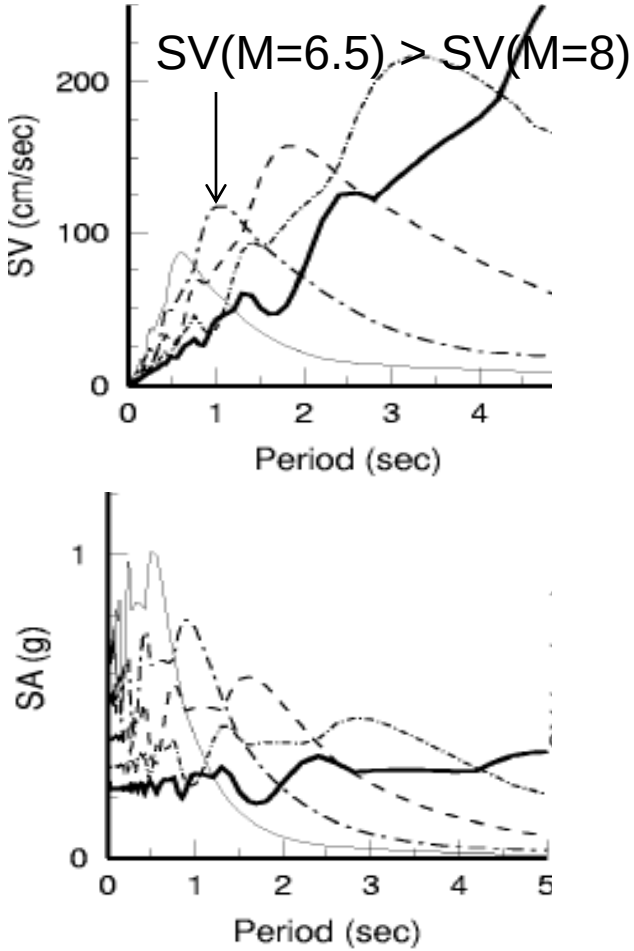

Baker (2007) algorithm

quantitative algorithm that uses wavelet analysis (Daubechies wavelet of order 4) to extract the largest velocity pulse from a given ground motion

Identifies pulse-like recordings calculating a score called *pulse indicator*:

$$\frac{1}{1+e^{-23.3+14.6(PGV_{ratio})+20.5(energy_{ratio})}}$$

Residual/original

I ≥ 0.85 '*pulse-like*'

I ≤ 0.15 '*non pulse-like*'

0.15 < *I* < 0.85 'ambiguous'

Two further conditions are added to exclude pulse-like signals likely not related to directivity:

-the 1st aims at the exclusion of late-arriving pulses (i.e. not occurring at the beginning of the signal);

-the 2nd aims at the exclusions of signals with PGV < 30 cm/s.

Signal decomposition

M_w6.3 L'Aquila Earthquake (AQG-SN)

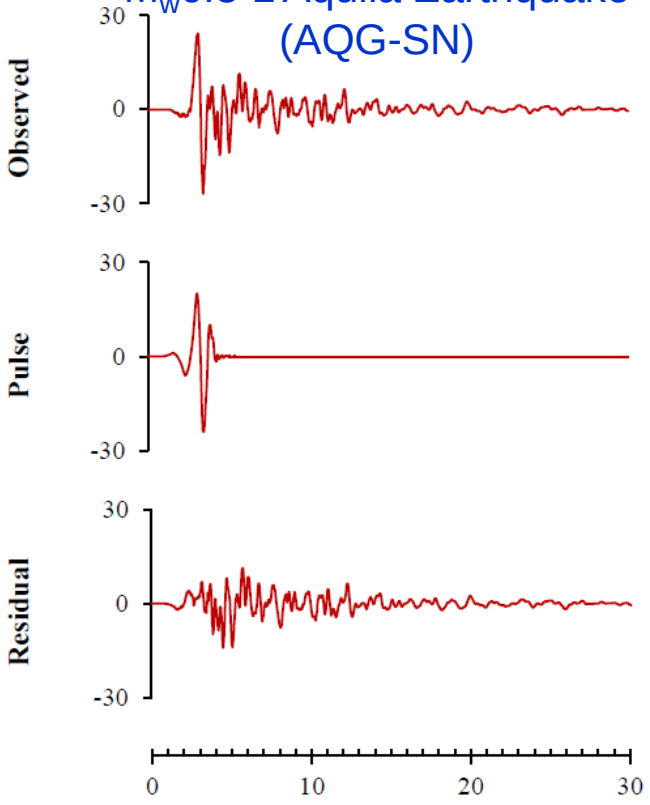

Case study: L'Aquila
April, 6 2009 strong-motion data

60x2 recordings (ITACA) corrected, rotated to SN and SP and analysed using Baker (2007) algorithm

(strike-angle assumed=142° Chioccarelli and Iervolino, 2012)

Station code	Ep. Dist (km)	Pulse Indicator	PGV (cm/s)	Late (0=no, 1=yes)	Is impulse? (0=no, 1=yes)	T_p (s)	Pulse indicator	PGV (cm/s)	Late (0=no, 1=yes)	Is impulse? (0=no, 1=yes)	T_p (s)
		SP					SN				
ANT	23.0	0.01	1.97	0	0	2.32	0.00	2.22	0	0	0.95
AQA	4.6	0.00	20.20	0	0	0.62	0.95	28.58	0	0	0.74
AQG	4.4	0.69	26.21	0	0	1.11	1.00	34.11	0	1	1.02
AQK	5.7	0.00	15.92	1	0	1.22	1.00	44.68	0	1	1.99
AQU	6.0	0.20	21.51	0	0	1.28	1.00	34.25	0	1	0.99
AQV	4.9	0.85	30.84	0	1	1.07	0.71	37.33	0	0	0.53
ASS	101.7	0.00	0.33	0	0	5.66	0.00	0.47	1	0	5.16
AVL	198.1	0.02	0.33	1	0	6.80	0.00	0.38	1	0	5.05
AVZ	34.9	0.01	9.83	1	0	1.61	0.98	13.04	1	0	1.88
BBN	199.6	0.02	0.29	1	0	5.64	0.00	0.19	1	0	5.08
BDT	178.8	0.05	0.42	0	0	4.17	0.00	0.39	1	0	3.54

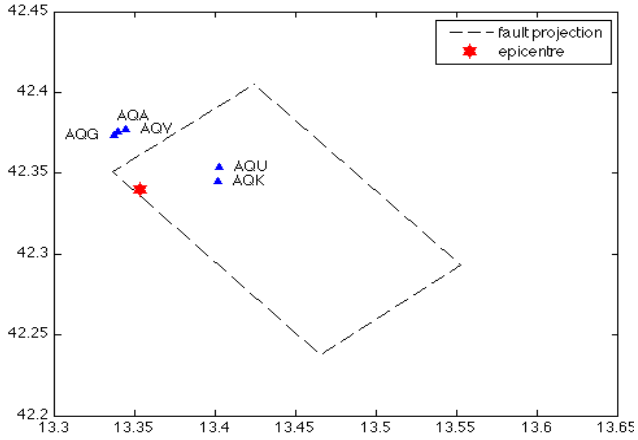

- Identified 5 impulsive recordings with Joyner & Boore distance < 2 Km
- Pulse mainly observed on SN component

Case study: L'Aquila
April, 6 2009 strong-motion data

Comparison with design response spectra

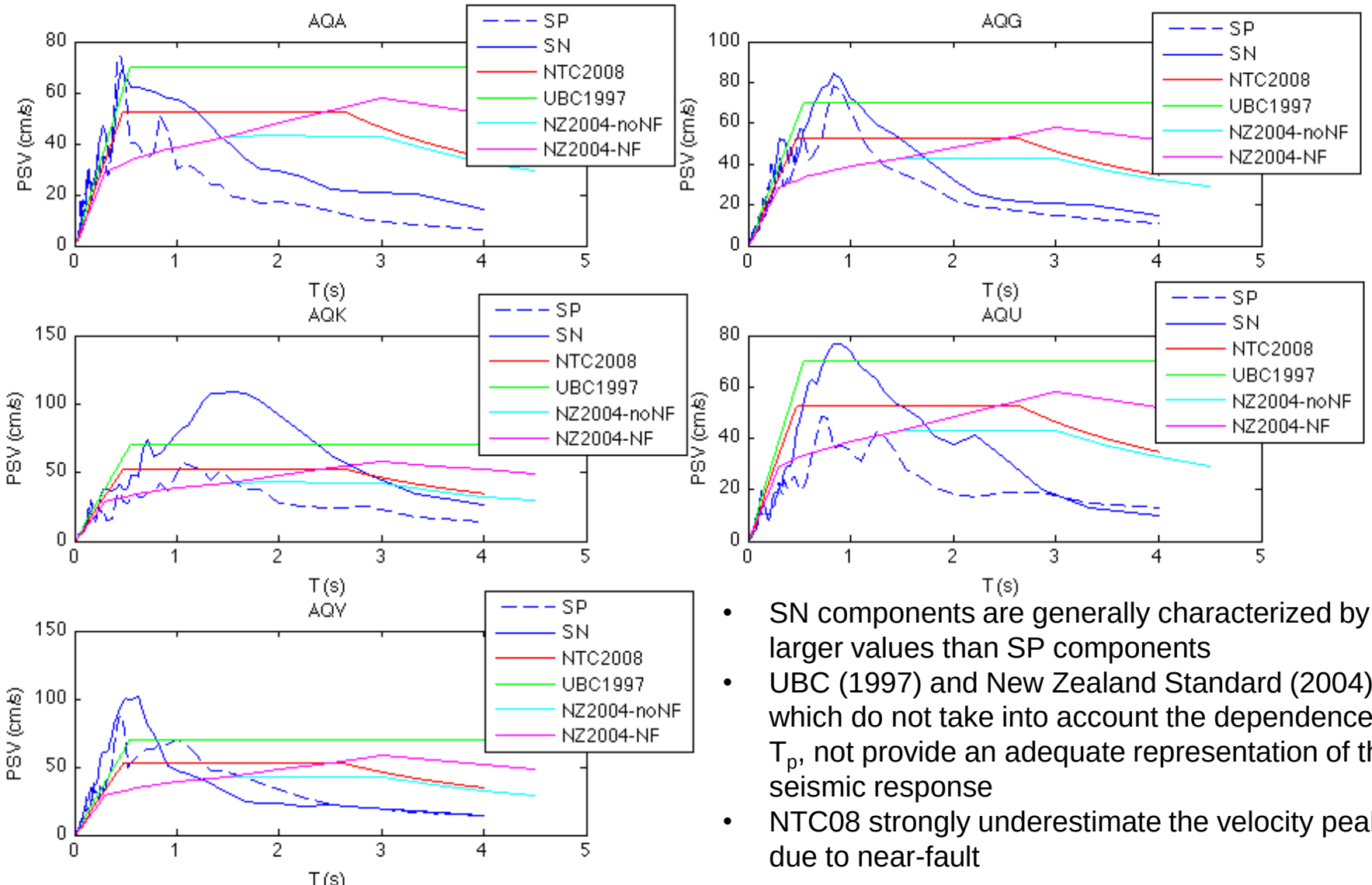

- SN components are generally characterized by larger values than SP components
- UBC (1997) and New Zealand Standard (2004), which do not take into account the dependence on T_p, not provide an adequate representation of the seismic response
- NTC08 strongly underestimate the velocity peaks due to near-fault

Proposal of a model to take into account near-fault effects

near-source spectrum = spectrum of the residual ground-motion
+
spectrum of the pulse

near-source design response spectrum = design response spectrum
x
amplification due to the presence of a pulse

OBJECTIVE: computation of amplification function

INPUT data: near-fault strong motion database +
reference design response spectrum

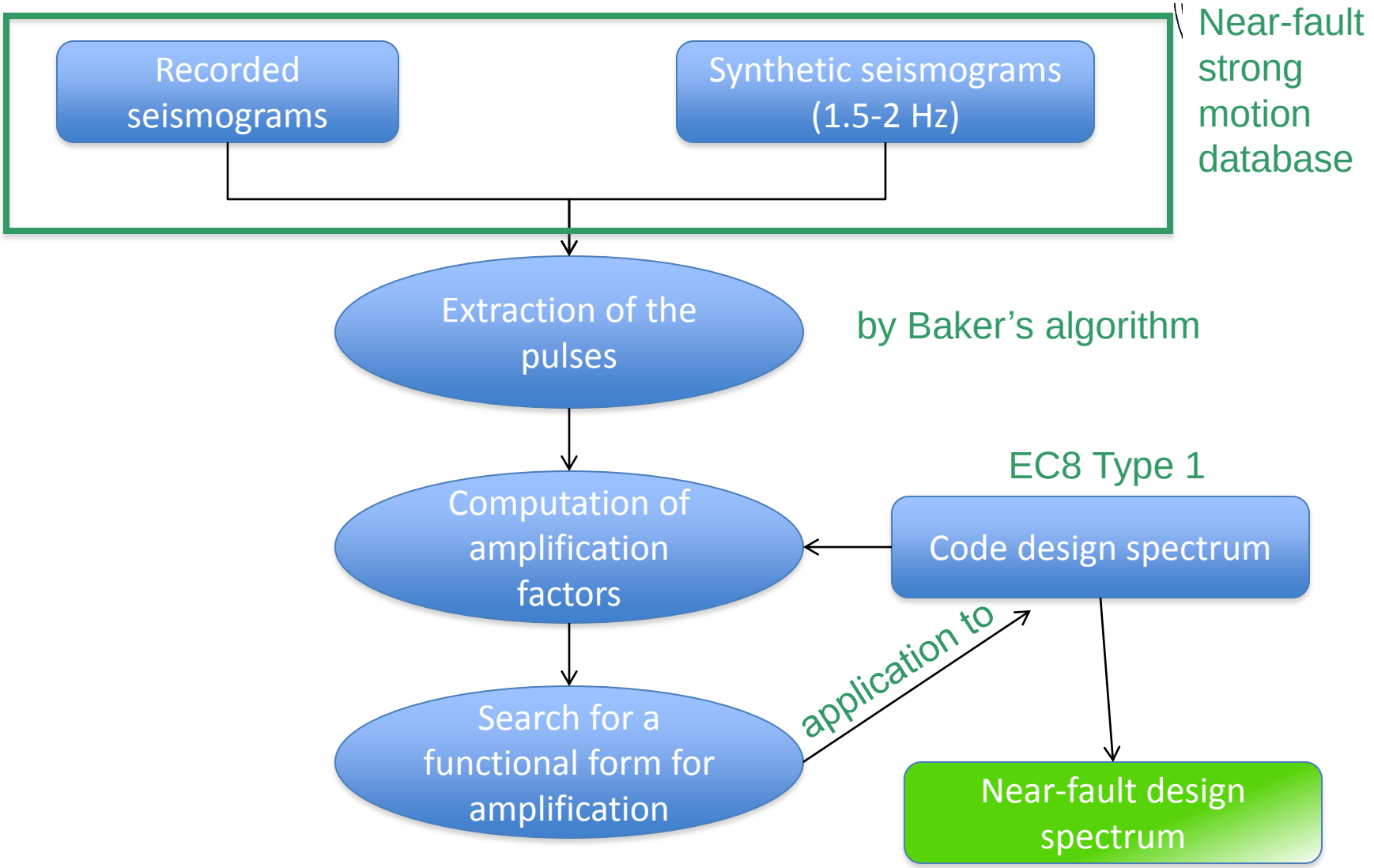
Recorded seismograms
Synthetic seismograms (1.5-2 Hz)
Near-fault strong motion database
Extraction of the pulses
by Baker's algorithm
EC8 Type 1
Computation of amplification factors
Code design spectrum
application to
Search for a functional form for amplification
Near-fault design spectrum

Recorded seismograms

- Shallow earthquakes
- $6.0 \leq M_w \leq 7.5$
- $0 < D < 15$ km increasing with M
- generic rock sites ($V_s30 > 600$ m/s, Geomatrix classification, Abrahamson and Silva, 1997)

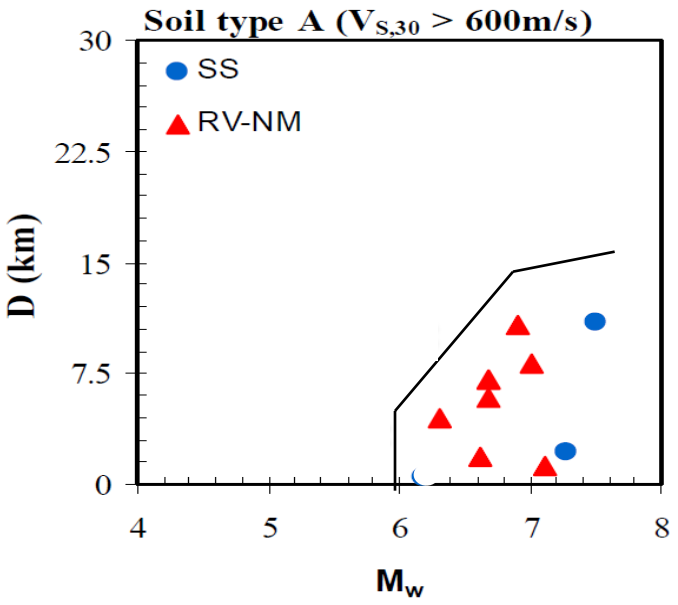

10 recordings

Earthquake	Date	Station code	PGV (cm/s)	M_w	D (km)	Fault type	$V_{S,30}$ (cm/s)
San Fernando	1971	Pacoima Dam (upper left abut)	122	6.6	1.8	RV	2016
Northridge	1994	Pacoima Dam (downstr)	50	6.7	7.0	RV	2016
Northridge	1994	Pacoima Dam (upper left)	107	6.7	7.0	RV	2016
Irpinia, Italy	1980	Sturno	41	6.9	10.8	NM	1000
L'aquila	2009	AQG	34	6.3	4.4	NM	1000
Kocaeli, Turkey	1999	Gebze	52	7.5	10.9	SS	792
Tabas, Iran	1978	tab	122	7.1	1.2	RV	767
Cape Mendocino	1992	Petrolia	82	7.0	8.2	RV	713
Landers	1992	Lucerne	146	7.3	2.2	SS	685
Northridge	1994	LA Dam	77	6.7	5.9	RV	629

Synthetic seismograms

Hisada and Bielak (2003)

- Kinematic finite-source model
- Green's functions of layer half-space
- Low frequency method (1.5-2Hz)
- T > 0.50-0.70s

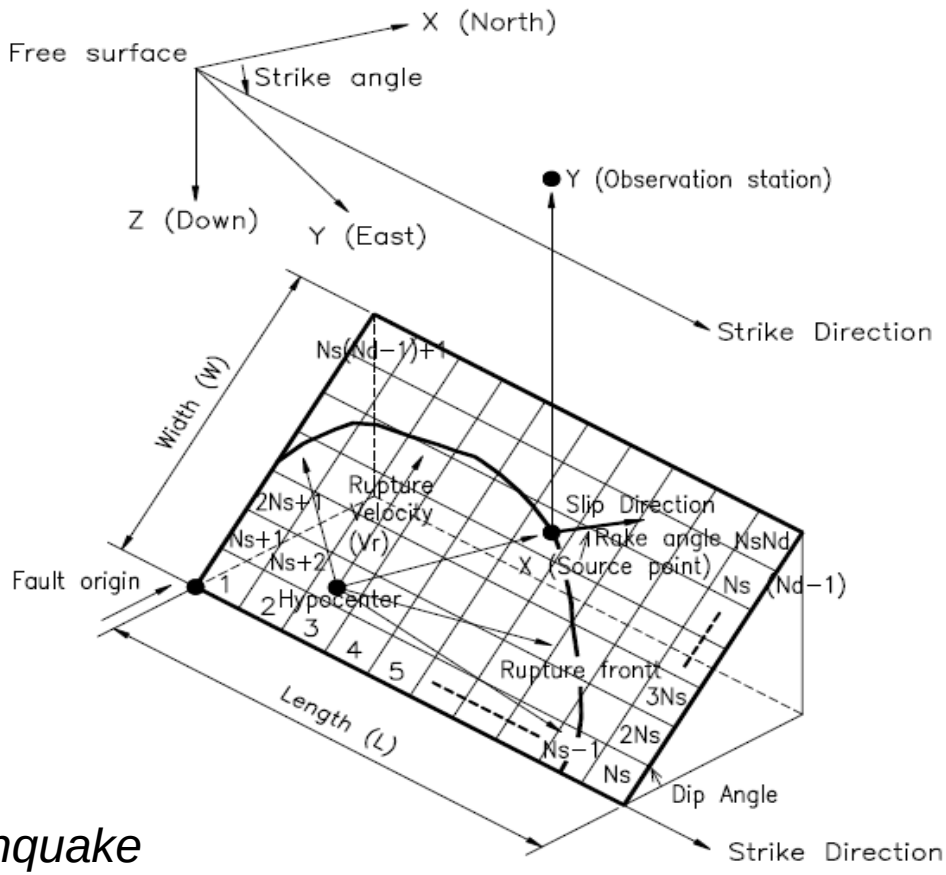

Validation

M_w7.3 1992 Landers Earthquake

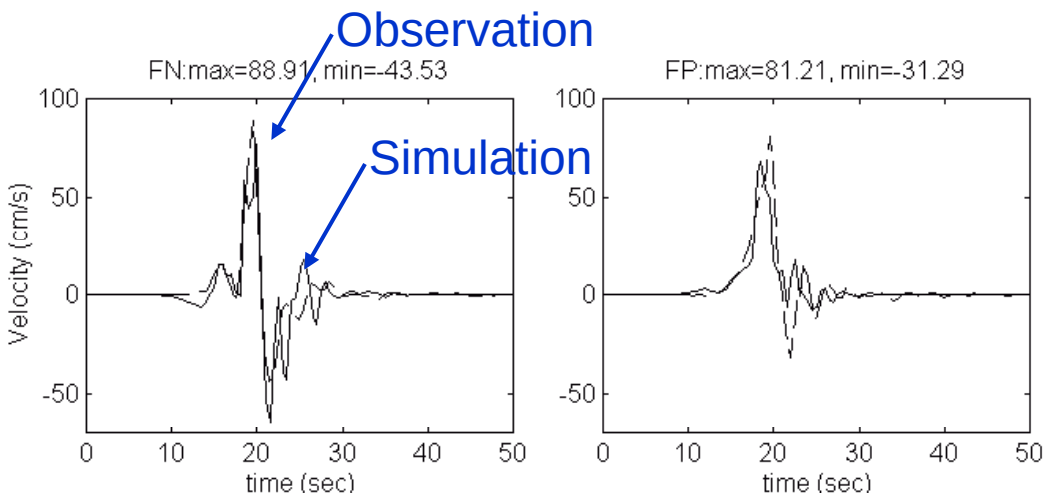

Hisada and Bielak (2004)

Synthetic seismograms

Random rupture depth $0<Z_0<5$km

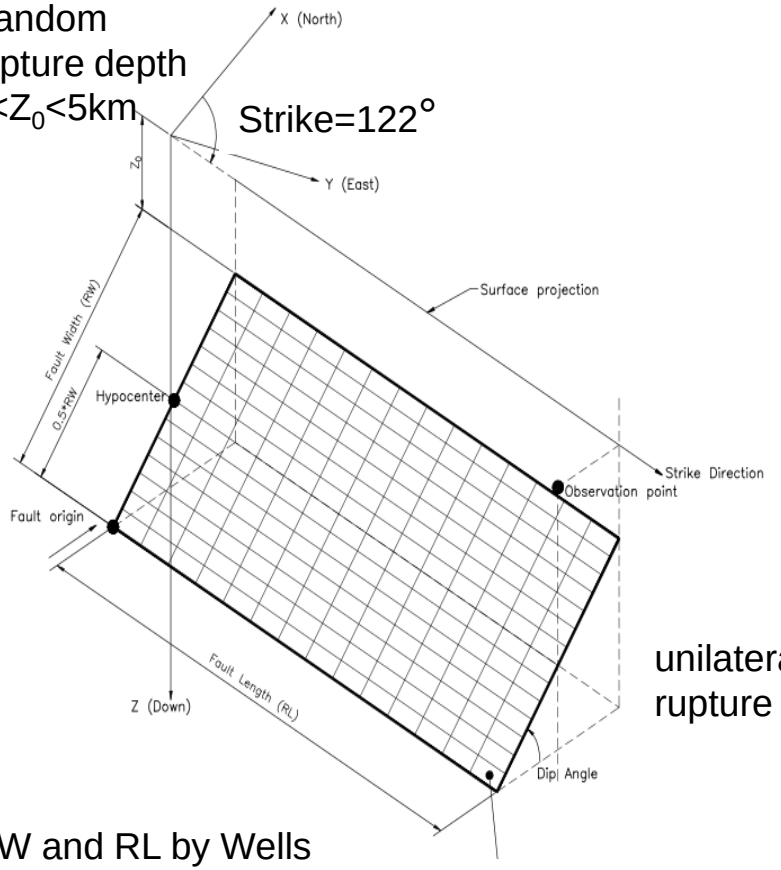

RW and RL by Wells and Coppersmith (1994)

unilateral rupture

14x14=196 subfaults
Random slip from 0m up to 1.90 x average displacement (by Wells and Coppersmith, 1994)

Northridge regional velocity structure (from Wald *et al.*, 1996).

V_P (km/s)	Q_P	V_S (km/s)	Q_S	Density (g/cm^3)	Thickness (km)	Depth (km)
1.9	100	1.0	50	2.1	0.5	0.0
4.0	200	2.0	100	2.4	1.0	0.5
5.5	400	3.2	200	2.7	2.5	1.5
6.3	400	3.6	200	2.8	23.0	4.0
6.8	600	3.9	300	2.9	13.0	27.0
7.8	600	4.5	300	3.3	-	40.0

V_r= 3.0km/s

Strike-slip faults: Rake: 0°, dip: 90°
Dip-slip faults: Rake 90°, dip: 40°

26 synthetics

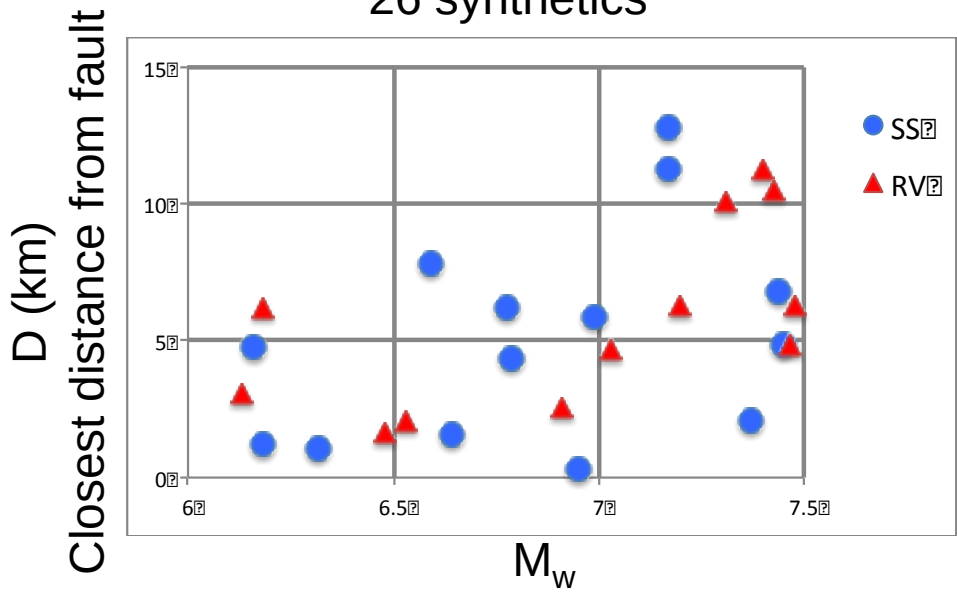

Near-fault strong motion database

Unified database: 10 recordings + 26 synthetics = 36 recordings

- 16 SS
- 20 RV-NM

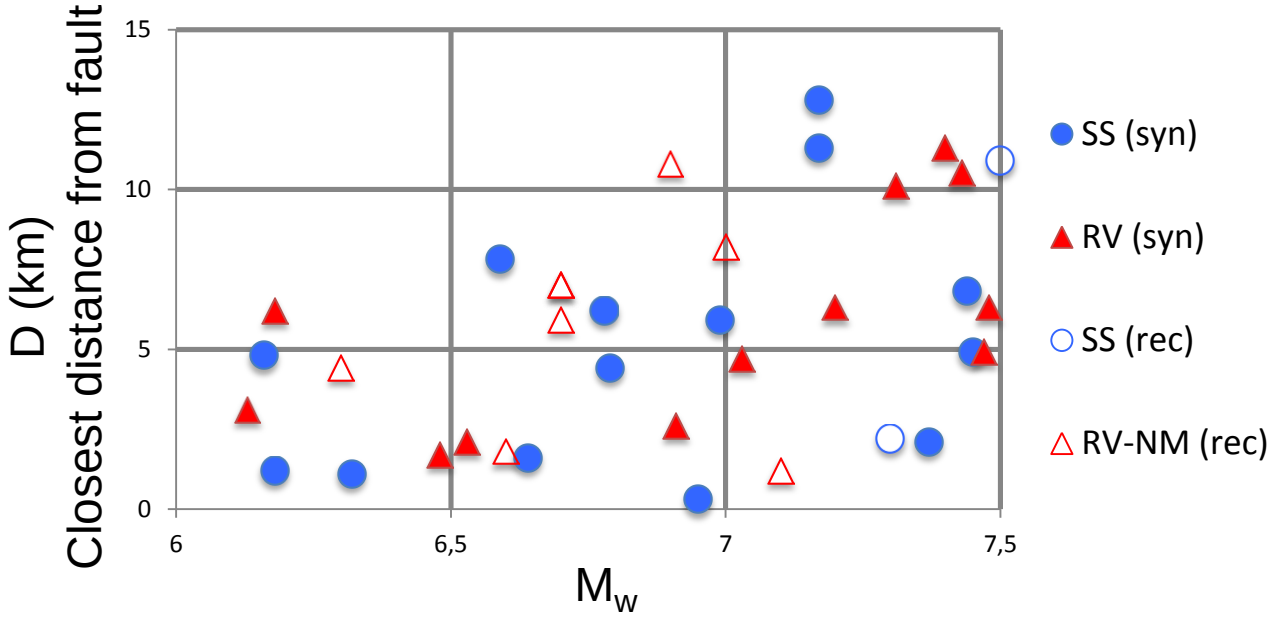

Extraction of the pulse

Recordings (real earthquakes):

	Strike-parallel					Strike-normal				
Station Code	Pulse Ind.	PGV (cm/s)	Late N, Y	Pulse N, Y	T_P (s)	Pulse Ind.	PGV (cm/s)	Late N, Y	Pulse N, Y	T_P (s)
AQG	0.8	21	N	N	1.1	1.0	27	N	N	1.0
pul	0.2	44	N	N	6.1	1.0	122	N	Y	1.6
LDM	0.5	43	Y	N	2.6	1.0	73	N	Y	1.6
PAC	0.0	19	Y	N	1.1	0.9	50	N	Y	0.9
PUL	0.8	50	Y	N	0.5	1.0	107	N	Y	0.9
STU	1.0	39	N	Y	2.5	1.0	38	N	Y	2.9
lcn	0.8	107	N	N	11.5	1.0	146	N	Y	6.3
tab	0.8	111	N	N	3.0	1.0	122	N	Y	6.1
GBZ	0.0	67	N	N	5.9	1.0	52	N	Y	5.9
PET	1.0	61	N	Y	1.0	0.9	82	N	Y	3.0

Neglected the limit on PGV

pulse in SN components for SS and dip-slip faults

Extraction of the pulse

Synthetics: pulse in SN for SS, SP for RV (rake=90°)

SS	Strike-parallel					Strike-normal				
	Pulse Ind.	PGV (cm/s)	Late N, Y	Pulse N, Y	T_P (s)	Pulse Ind.	PGV (cm/s)	Late N, Y	Pulse N, Y	T_P (s)
Syn-01	1	9	N	N	3.1	1	36	N	Y	2.5
Syn-02	1	22	N	N	2.6	1	41	N	Y	2.6
Syn-11	0	0.1	Y	N	0.3	1	73	N	Y	4.5
Syn-12	0	0.1	N	N	5.4	1	83	N	Y	5
Syn-13	0.9	17	N	N	4	1	46	N	Y	5.3
Syn-16	1	20	N	N	4.3	1	44	N	Y	5.6
Syn-17	1	18	N	N		1	39	N	Y	5.1
Syn-18	0	0.3	Y	N		1	123	N	Y	6.4
Syn-19	0	1	N	N		1	240	N	Y	5.5
Syn-22	1	91	N	Y		1	135	N	Y	6.7
Syn-26	1	50	Y	N	4.1	1	66	N	Y	6.6
Syn-28	1	41	N	Y	4.9	1	48	N	Y	6.6
Syn-32	1	7	N	N	3.4	1	27	N	N	4.2
Syn-33	1	36	N	Y	3.3	1	59	N	Y	5.5

Neglected the limit on PGV

RV	Strike-parallel					Strike-normal				
	Pulse Ind.	PGV (cm/s)	Late N, Y	Pulse N, Y	T_P (s)	Pulse Ind.	PGV (cm/s)	Late N, Y	Pulse N, Y	T_P (s)
Syn-03	1	41	N	Y	3.5	1	23	N	N	2.6
Syn-05	1	42	N	Y	3.4	1	24	N	N	1.1
Syn-09	1	33	N	Y	3.7	1	28	Y	N	3.4
Syn-14	1	75	N	Y	3.5	1	45	N	Y	1.2
Syn-15	1	126	N	Y	3.4	1	53	N	Y	1.8
Syn-20	1	72	N	Y	4.2	1	30	N	Y	2.9
Syn-21	1	187	N	Y	4.9	1	133	N	Y	4.8
Syn-24	1	95	N	Y	5.3	1	78	N	Y	3.9
Syn-25	1	155	N	Y	5.3	1	72	N	Y	4.4
Syn-29	1	80	N	Y	6.1	0.9	58	Y	N	4.1
Syn-30	1	88	N	Y	5.9	1	52	N	Y	5.1
Syn-31	1	54	N	Y	6	1	29	Y	N	4.7

Extracted pulses (recordings + synthetics)

$6.0 < M_w \leq 6.5,\ 0 < D \leq 5$km

Syn-32(SS) Syn-01(SS) Syn-02(SS) AQG(NM) Syn-03(RV) Syn-05(RV) Syn-09(RV)

$6.5 < M_w \leq 7.0,\ 0 < D \leq 5$km

Syn-11(SS) Syn-12(SS) Syn-13(SS) pul(RV) Syn-14(RV) Syn-15(RV)

$6.5 < M_w \leq 7.0,\ 5 < D \leq 10$km

Syn-33(SS) Syn-16(SS) Syn-17(SS) LDM(RV) PAC(RV) PUL(RV) STU(NM)

Extracted pulses (recordings + synthetics)

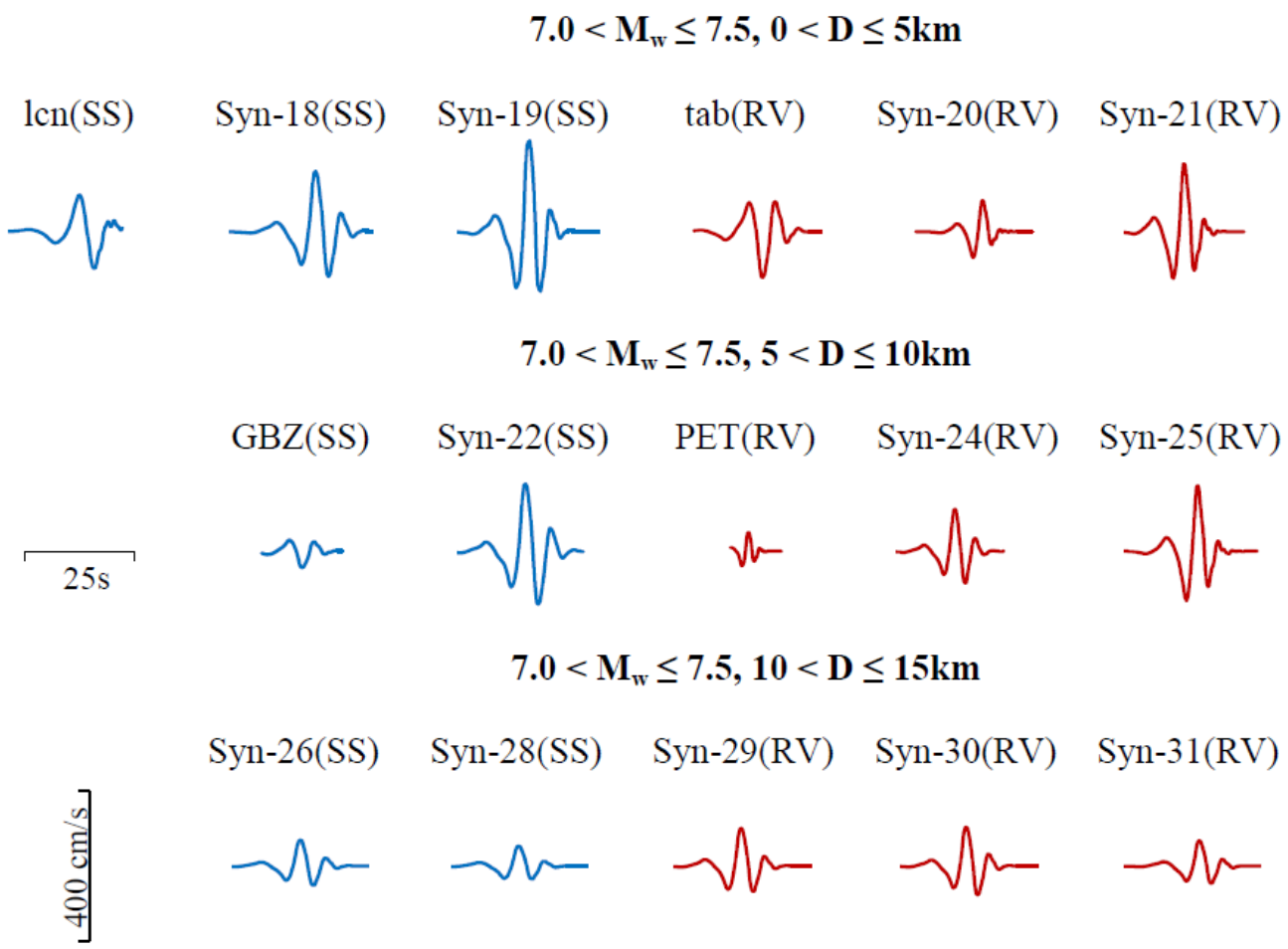

Code design spectrum

EC8 elastic response spectrum (ξ 5%, Type 1, rock site, a_g= 0.35g)

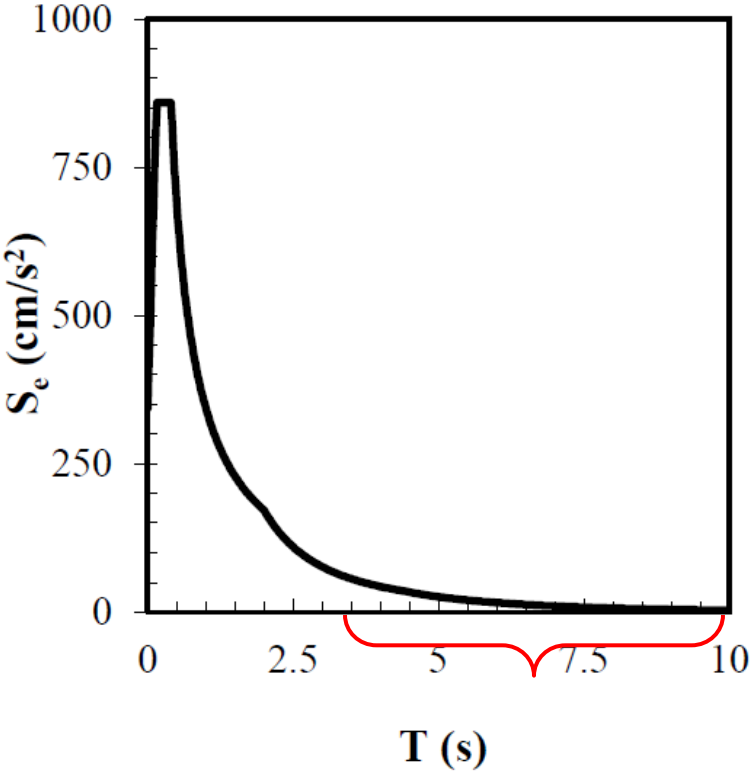

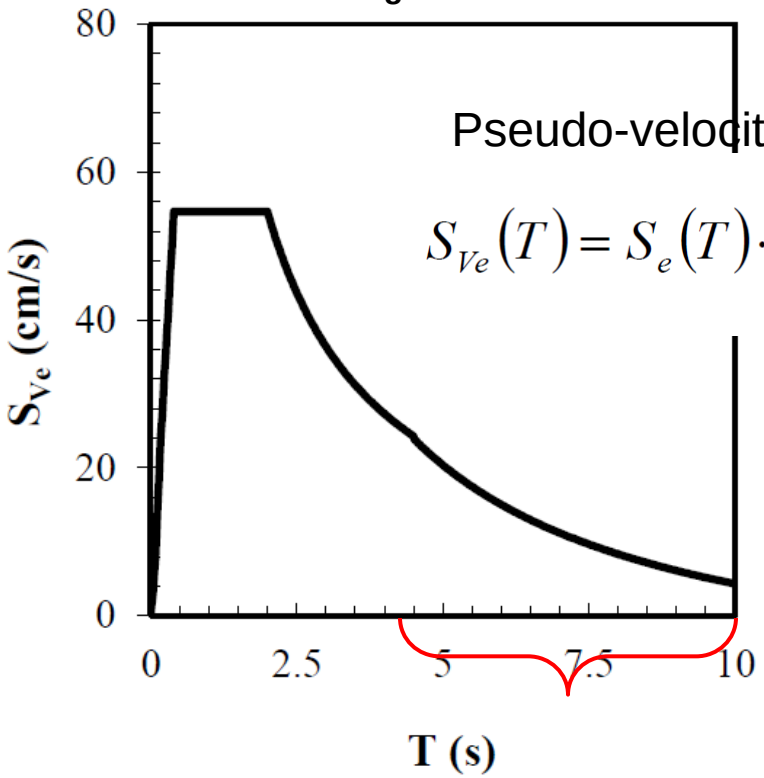

Pseudo-velocity

$$S_{Ve}(T) = S_e(T) \cdot \left[\frac{T}{2 \cdot \pi}\right]$$

EC-8 Section 3.2.2.2(6):

NOTE For the Type 1 elastic response spectrum referred to in Note 1 to **3.2.2.2(2)**P, such a definition is presented in Informative Annex A in terms of the displacement response spectrum. For periods longer than 4,0 s, the elastic acceleration response spectrum may be derived from the elastic displacement response spectrum by inverting expression (3.7).

Amplification factors

Response spectra of original signals + EC8

Response spectra of pulses + EC8

$$A_f = \frac{PSv_{pulse}}{PSv_{EC-8}}$$

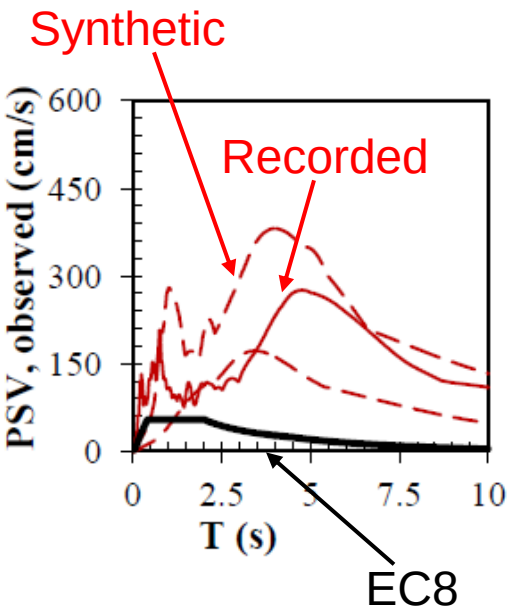

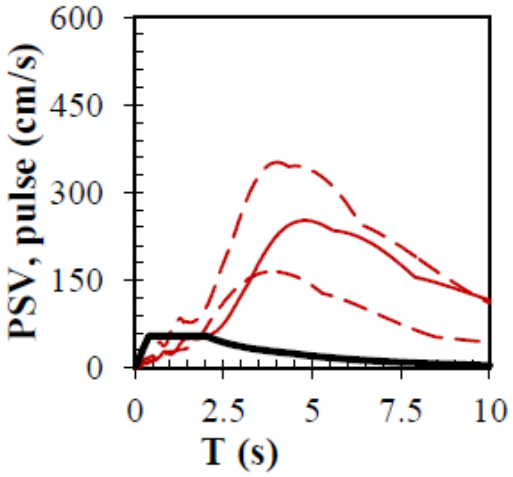

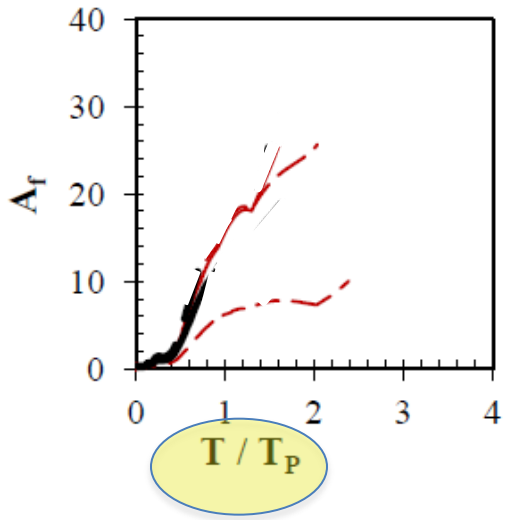

Normalized structural period

Dip-slip faults, $7.0 < M_w \leq 7.5$, $0 < D \leq 5$km

Functional form

$A_f = f(D, M_w, T/T_P)$

$$f(D) = d \cdot D + g$$

Influence of distance

Strike-slip (SN)

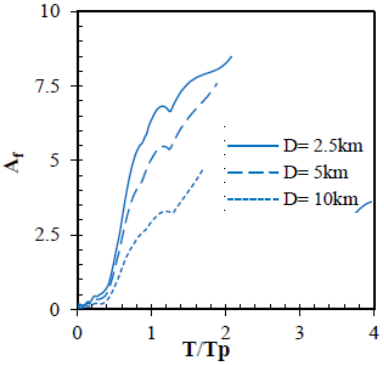

Reverse (SP)

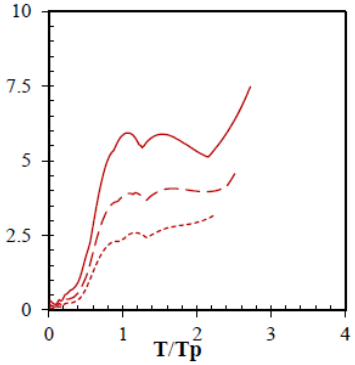

M_W=6.75
D=2.5, 5, 10 km

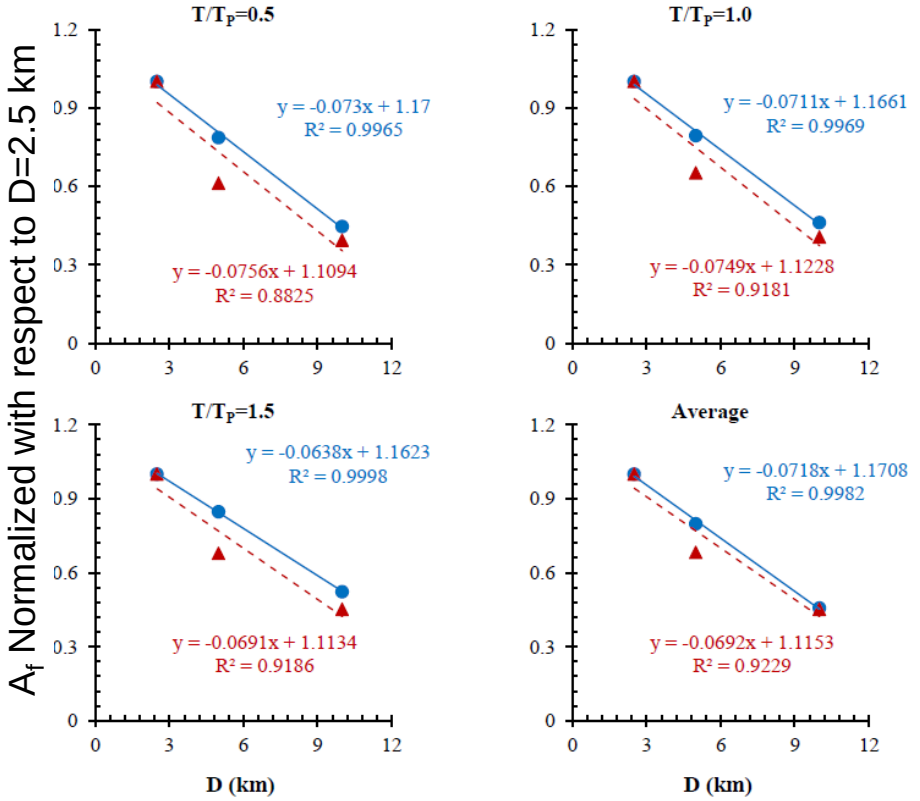

Functional form

$A_f=f(D,M_w,T/T_P)$

$$f(M_w)=b\cdot e^{c\cdot M_w}$$

Influence of magnitude

Strike-slip (SN)

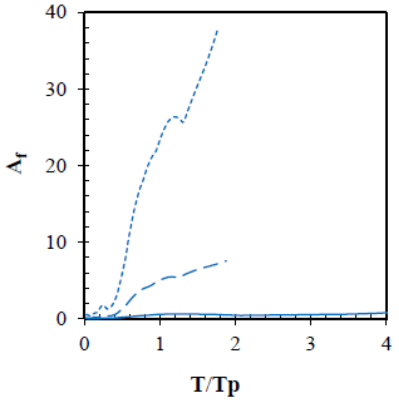

Reverse (SP)

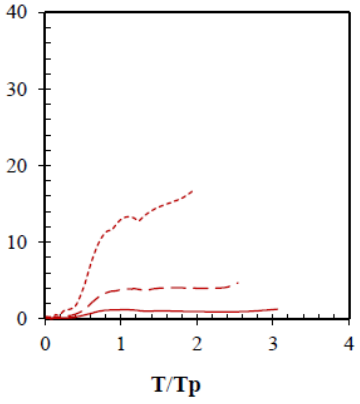

M_W=6.25, 6.75, 7.25
D=5km

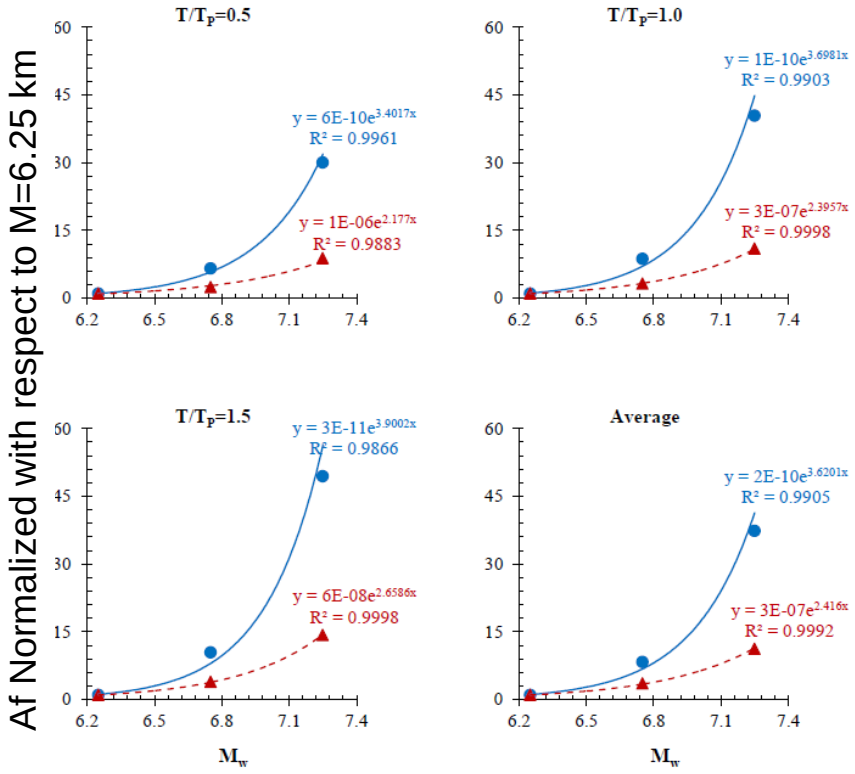

Functional form

$A_f=f(D,M_w,T/T_P)$

Influence of focal mechanism

M_w=6.75
D=2.5,5,10 km

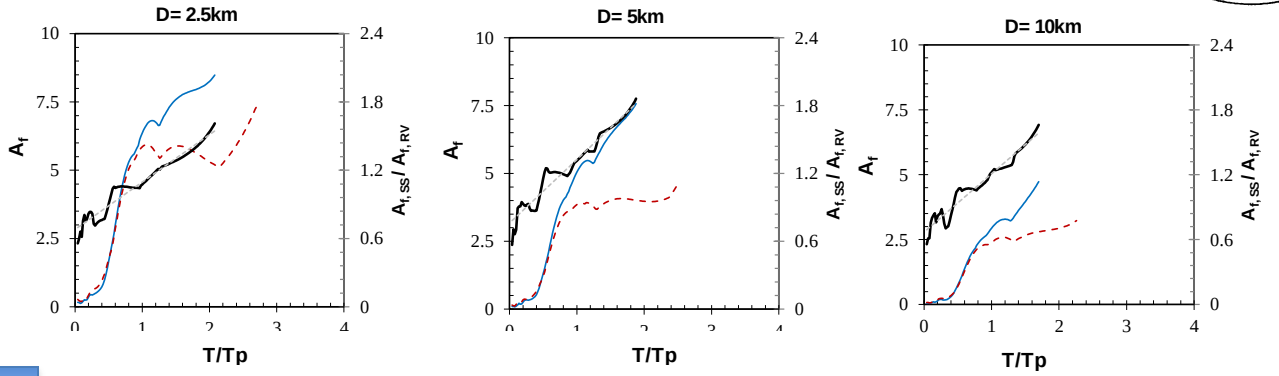

Different calibration of coefficients of amplification function for SS and RV-NM

T/T_P<0.7s: SS≈RV
T/T_P>0.7s: SS>RV with difference increasing with T/T_P

M_w=6.25,6.75,7.25
D=5 km

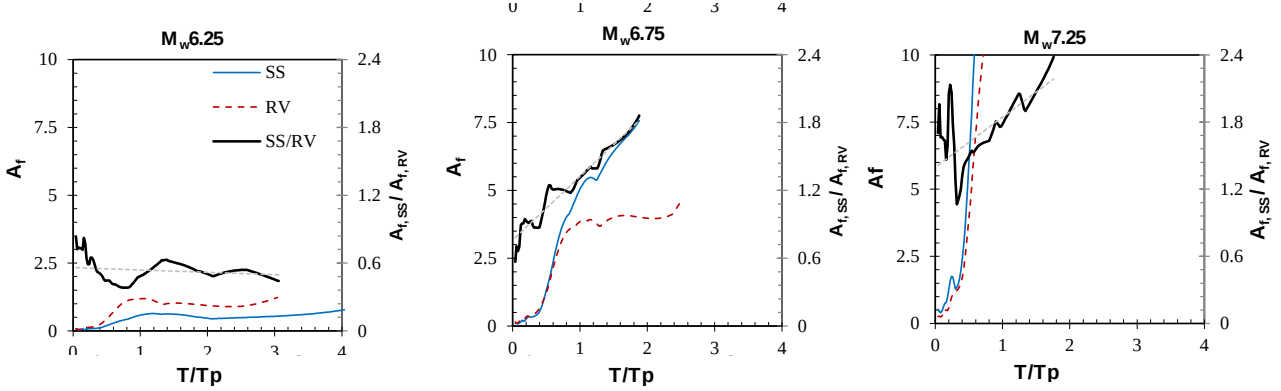

behavior dependent on M_w
T/T_P<0.4s: SS≈RV
T/T_P>0.4s: RV>SS reaching with constant value for 1<T/T_P<3s (M_w=6.25)
SS>RV with difference increasing with T/T_P (M_w=6.75,7.25)

Functional form

$A_f = f(D, M_w, T/T_P)$

$$A_f = a \cdot \left(b \cdot e^{c \cdot M_w}\right) \cdot \left(d \cdot D + g\right) \geq 1.0$$

Coefficients estimated for different T/T_P by multi-step regression (3 steps)

T/T_P	a	b	c	d	g	ε	σ(ε)
0.1	0.238	1.14E-01	0.313	-0.032	1.187	0.988	0.938
0.3	0.635	6.70E-04	1.043	-0.071	1.473	0.935	0.459
0.5	2.091	1.41E-05	1.586	-0.077	1.533	0.919	0.366
0.7	5.163	2.87E-06	1.809	-0.080	1.563	0.900	0.361
1.0	8.018	1.28E-06	1.924	-0.083	1.572	0.867	0.354
1.4	9.914	4.73E-07	2.063	-0.088	1.627	0.820	0.417
2.2	3.062	9.80E-08	2.407	-0.155	1.901	0.872	0.484
3.0	2.547	1.89E-09	2.999	-0.155	2.146	0.658	0.477
4.0	0.829	1.77E-04	1.308	-0.238	2.313	0.930	0.522

All focal mechanism:

Step 1: estimate of *a*
Step 2.1: estimate of *b* and *c*
Step 3.1: estimate of *d* and *g*

		Dip-slip				Strike-slip					
T/T_P	a	b	c	d	g	b	c	d	g	ε	σ(ε)
0.1	0.238	2.667	-0.112	0.003	0.977	2.92E-06	1.750	-0.108	1.725	1.023	0.701
0.3	0.635	4.67E-03	0.786	-0.056	1.370	3.50E-06	1.750	-0.103	1.688	0.939	0.347
0.5	2.091	1.43E-04	1.263	-0.054	1.376	8.87E-07	1.971	-0.093	1.621	0.926	0.377
0.7	5.163	4.13E-06	1.750	-0.063	1.465	6.70E-07	2.016	-0.092	1.624	0.932	0.384
1.0	8.018	1.78E-06	1.865	-0.064	1.476	1.23E-06	1.942	-0.089	1.594	0.880	0.368
1.4	9.914	1.47E-07	2.203	-0.063	1.465	1.70E-06	1.906	-0.089	1.599	0.848	0.403
2.2	3.062	3.20E-08	2.547	-0.175	2.057	3.98E-07	2.268	-0.027	1.133	0.964	0.688
3.0	2.547	1.05E-09	2.999	0.021	0.817	3.77E-09	2.999	0.075	0.565	0.944	0.363
4.0	0.829	1.77E-04	1.308	-0.238	2.313	1.77E-04	1.308	-0.238	2.313	0.930	0.522

Dip-slip and strike-slip separately:

Step 2.2: estimate of *b* and *c*
Step 3.2: estimate of *d* and *g*

Application

$$S_e(A_f, T) = A_f(D, M_w, T) \cdot S_e(T)$$

Near-fault design specrum

- Narrow band model
- Peak close to the pulse period
- Period increasing with magnitude

EC8

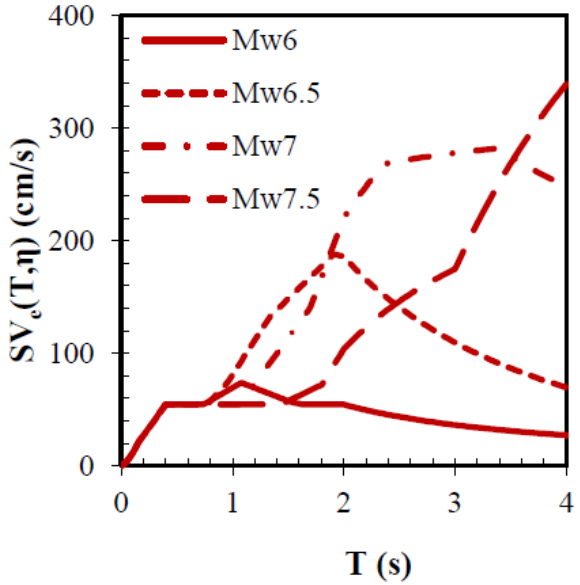

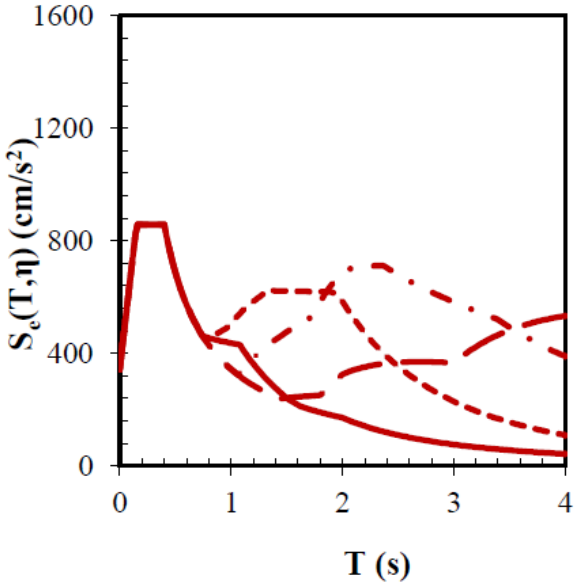

$T_{P(M6.0)}$= 1.1s
$T_{P(M6.5)}$= 1.9s
$T_{P(M7.0)}$= 3.4s
$T_{P(M7.5)}$= 6.0s

Design spectra for a reverse-slip fault, distance D= 2.5km

Comparison with recorded response spectra

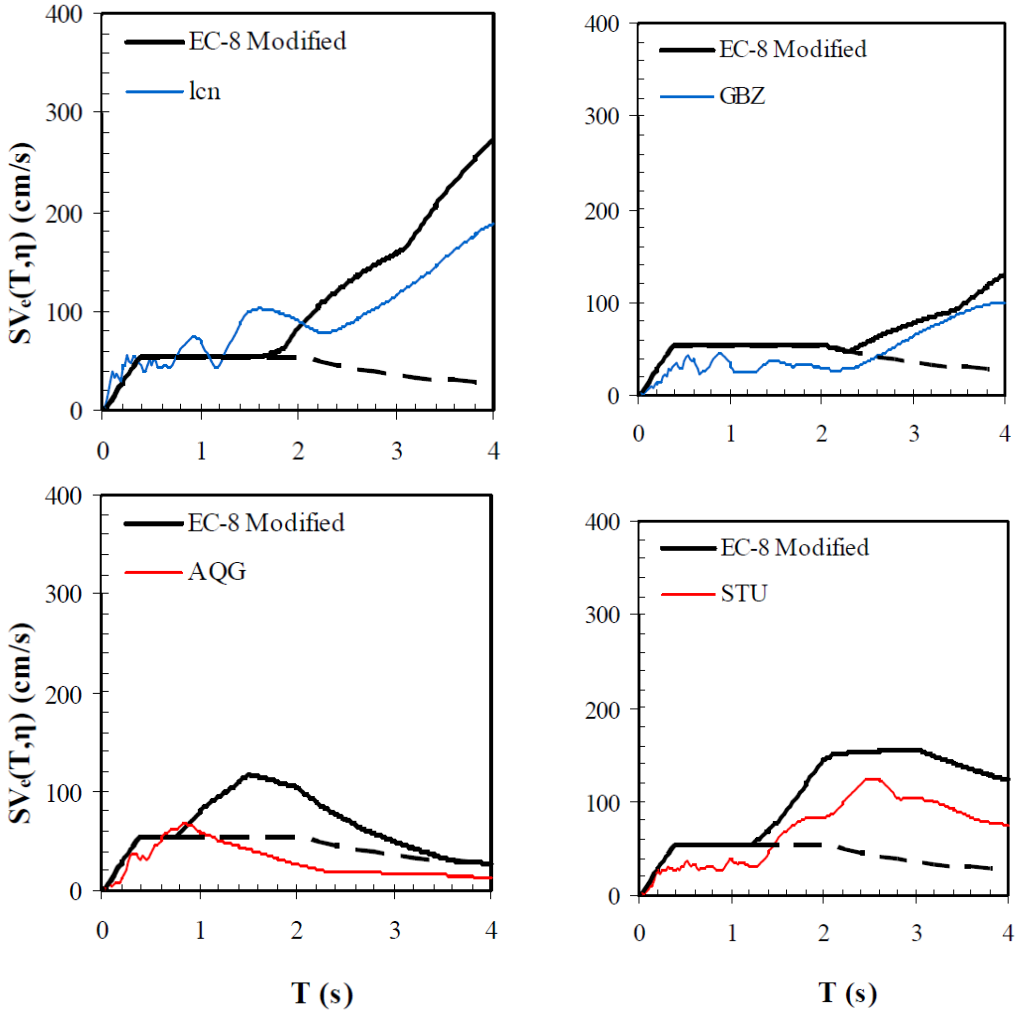

Application for seismic design

$$S_e\left(A_f, T\right) = A_f\left(D, M_w, T\right) \cdot S_e\left(T\right)$$

site of interest

Application for seismic design

$$S_e\left(A_f, T\right) = A_f\left(D, M_w, T\right) \cdot S_e\left(T\right)$$

Only for buildings in Zone 1: ag=0.35 g
Type 1 EC8
Ground Type A
□=5%

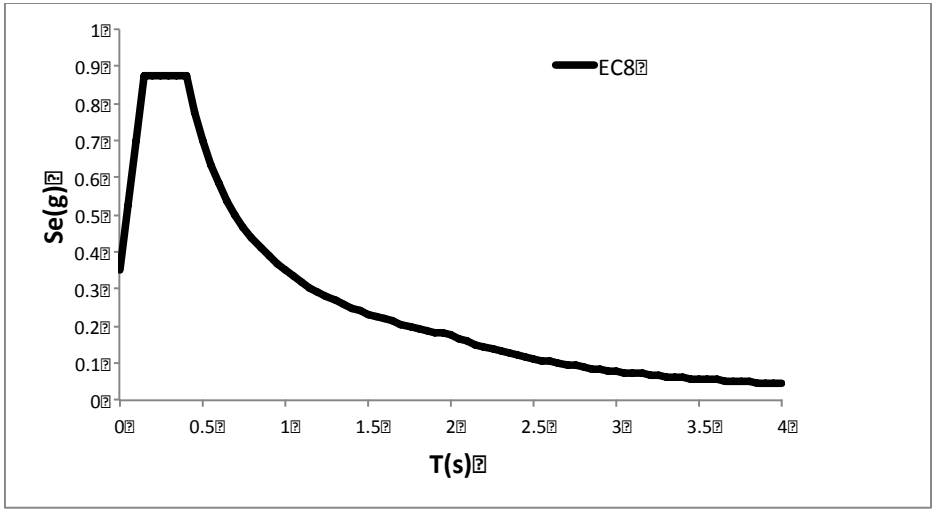

Application for seismic design

$$S_e(A_f, T) = A_f(D, M_w, T) \cdot S_e(T)$$

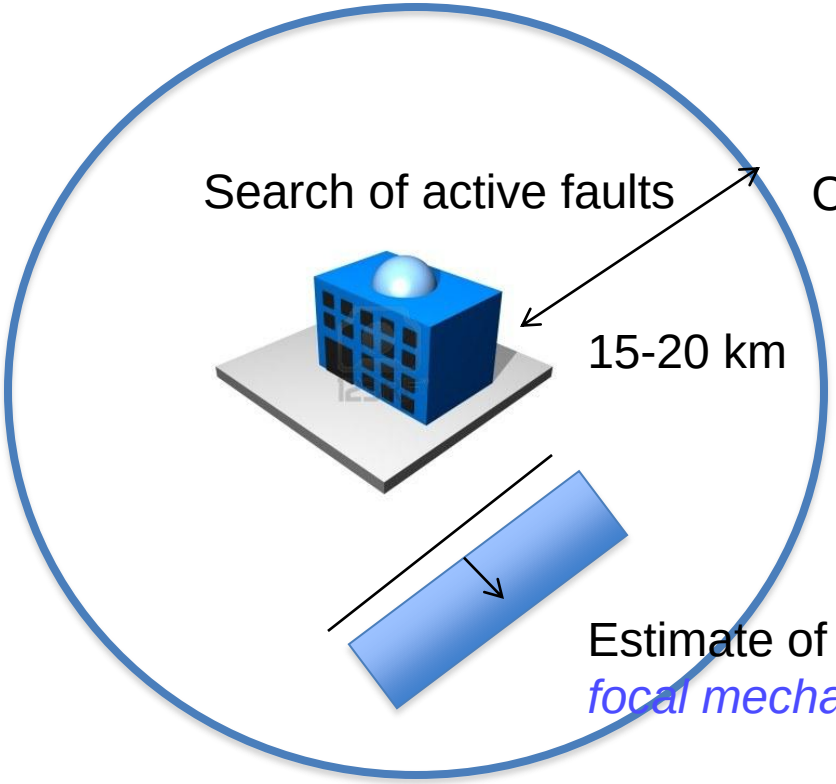

Computation of amplifications dependent on T/T_P

$$A_f = a \cdot \left(b \cdot e^{c \cdot M_w}\right) \cdot \left(d \cdot D + g\right) \geq 1.0$$

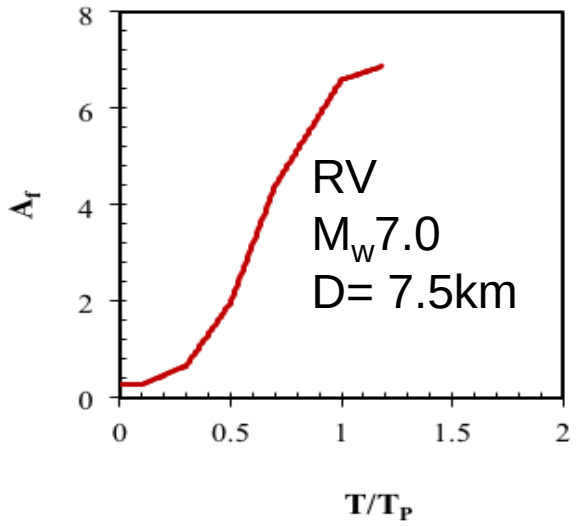

Application for seismic design

$$S_e\left(A_f, T\right) = A_f\left(D, M_w, T\right) \cdot S_e\left(T\right)$$

Estimate of the pulse period from M_w

Strike-slip fault: $\ln\left(T_P\right) = -2.355 + 0.573 \cdot M_w$

Dip-slip fault: $\ln\left(T_P\right) = -6.795 + 1.145 \cdot M_w$

All-fault types: $\ln\left(T_P\right) = -4.708 + 0.872 \cdot M_w$

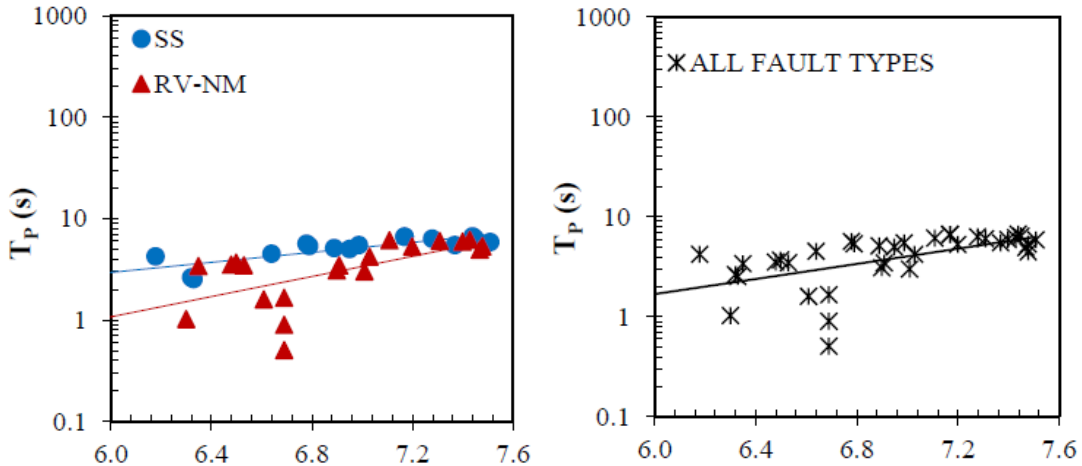

Application for seismic design

$$S_e\left(A_f, T\right) = A_f\left(D, M_w, T\right) \cdot S_e\left(T\right)$$

Estimate of the pulse period from M_w

Computation of amplifications dependent on T

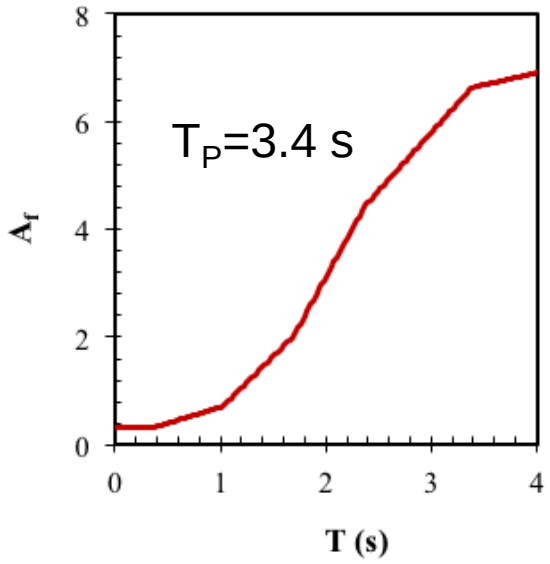

Application for seismic design

$$S_e\left(A_f, T\right) =$$

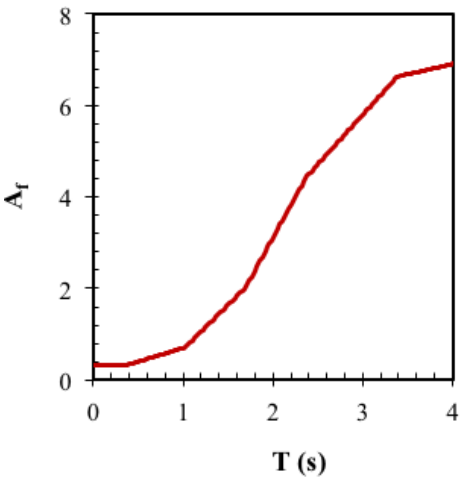

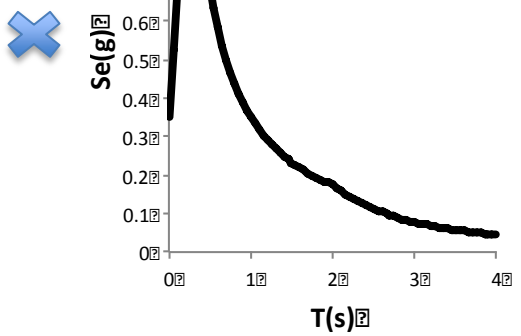

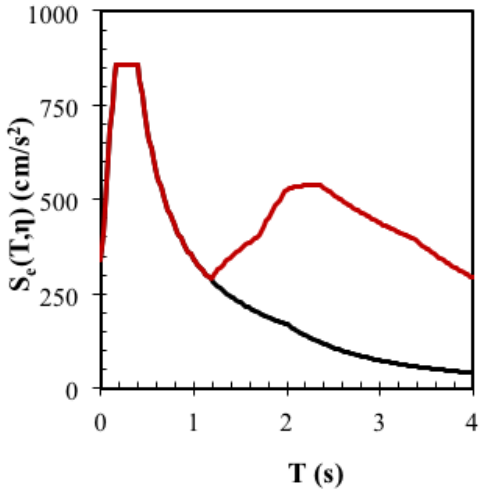

Amplified EC8

Conclusioni

RELUIS 2: proposta per tenere conto degli effetti near-source nella definizione dello spettro di risposta EC8-Tipo 1.

Nello specifico, è stata determinata una funzione di amplificazione capace di simulare gli effetti dell'impulso near-source, calibrata utilizzando dati reali e sintetici (in bassa frequenza).

Tale proposta necessita tuttavia di validazioni e approfondimenti.

ReLuis 3: Attività

- Sviluppo di un metodo consolidato ed affidabile per il calcolo di spettri near-fault su tutto il territorio nazionale.

- Completamento della banca dati near-fault integrando le registrazioni disponibili con i segnali ottenuti da simulazioni numeriche condotte in modo parametrico in modo da coprire le “lacune” dei segnali reali.

ReLuis 3: Attività pianificate per il primo anno

ATTIVITÀ

A.1) validazione e calibrazione dei codici di calcolo per la generazione di sismogrammi sintetici in condizioni near-source mediante simulazione del terremoto dell'Emilia del 20.05.2012 (stazione di Mirandola):

A.1.1) codice di calcolo in bassa freq. di Hisada-Bielak (2003)

A.1.2) codice di calcolo a banda larga sviluppato da UCSB e incluso nel BroadBand Platform(http://scec.usc.edu/scecpedia/Broadband_Platform).

A.2) contributo iniziale alla creazione di una banca dati di accelerogrammi reali e sintetici pienamente caratterizzata in termini di meta-dati per gli effetti near-source.

A.1.1 Low-frequency simulation of the 20 May 2012 Emilia earthquake

Hisada-Bileak (2003) simulation code

Detailed geological model (up to 11 km)

Numb. Of layers	Depth (m)	Density (t/m3)	Thickness (m)	Vp (m/s)	Qpo	Vs (m/s)	Qso
1	from 0 to -932	1.75	932	1700	28	981	19
2	from -932 to -1565	2.10	633	2500	37	1250	25
3	from -1565 to -2660	2.45	1095	3500	307	2050	205
4	from -2660 to -4560	2.60	1900	4500	388	2598	259
5	from -4560 to -9760	2.75	5200	5570	480	3200	320
6	from -9760 to -37252	2.90	27492	6928	600	4000	400
7	from -37252 to -50939	3.20	13687	7448	645	4300	430
8	from -50939 to -100939	3.25	50000	8183	708	4725	472
9	from -100939 to -150939	3.30	50000	7534	652	4350	435
10	from -150939 to -200939	3.35	50000	7707	667	4450	445
11	from -200939 to -250939	3.35	50000	7950	688	4590	459
12	from -250939 to -300939	3.40	50000	8054	697	4650	465
13	from -300939 to ∞	3.40	0	8227	712	4750	475

(from Toscani et al., 2009; Fantoni et al., 2010)

Le caratteristiche geologico-geotecniche locali saranno prese in considerazione mediante un’analisi di risposta sismica locale eseguita mediante un approccio di tipo stocastico sviluppato da EUCENTRE-UNIPV.

A.1.1 Low-frequency simulation of the 20 May 2012 Emilia earthquake

Hisada-Bileak (2003) simulation code

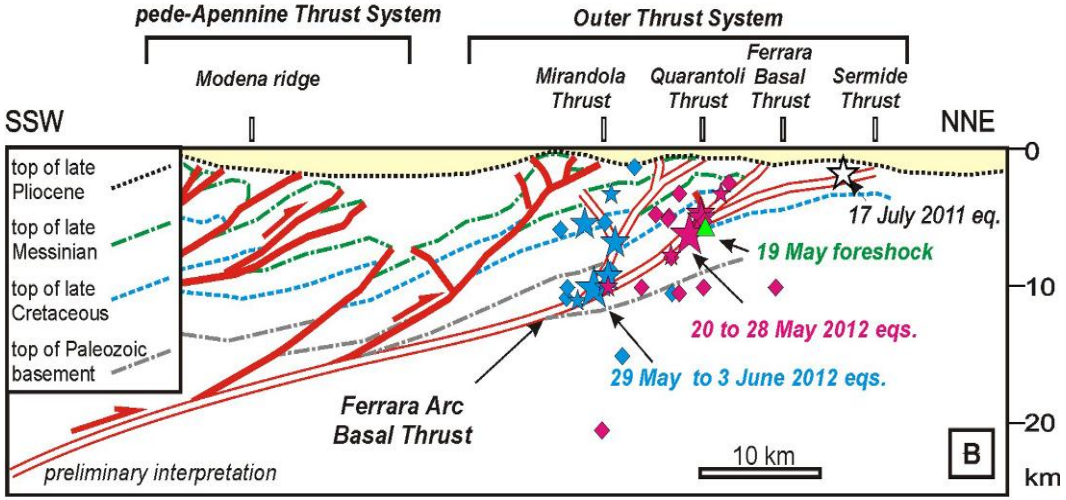

[modified from Toscani et al. 2009]

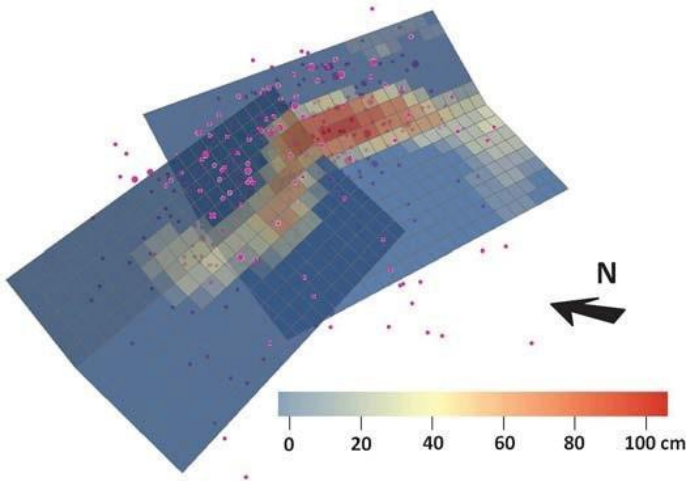

Slip distribution from Pezzo et al. 2013

A.1.2 Broadband simulation of the 20 May 2012 Emilia earthquake

Broadband ground motion simulation method
developed by University of California Santa Barbara (led by Prof. Archuleta)

Programs are included in the **Broadband Platform** (http://scec.usc.edu/scecpedia/Broadband_Platform), a software system which generates 0-10 Hz seismograms for historical and scenario earthquakes in California

Kinematic Source Modeling (SAL)

Definition of slip rate function for each point source

(Schmedes et al., JGR, 2010; GJI, 2013)

Functional form of slip rate parametrized by 4 source parameters:

- final slip
- local rupture velocity
- rise time
- peak time (is a measure of the impulsive part of the slip rate function)

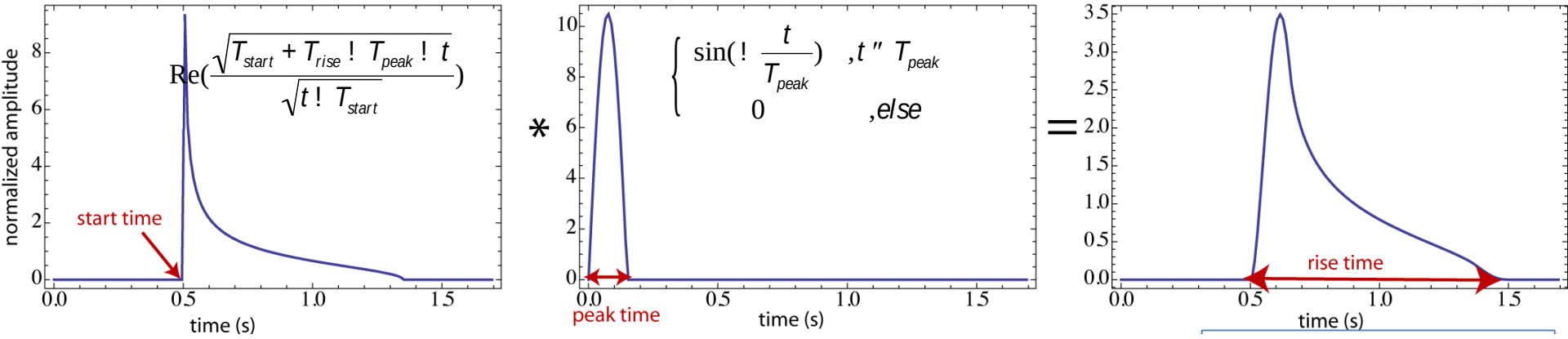

Convolution of slip rate function proposed by Nielsen and Madariaga (2003) with half sine (Madariaga, pers. Comm.)

Correlated random source parameters based on Dynamic Rupture Models (Schmedes et al., JGR, 2010; GJI, 2013)

Computed/Collected many (>300) spontaneous dynamic ruptures for a variety of initial models.

how are amplitudes distributed?

marginal distributions

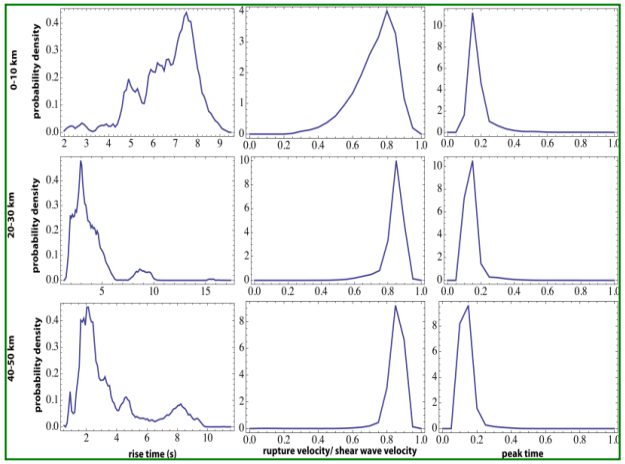

which are allowed to change as a function of distance from the hypocentre

what is the spatial distribution of the parameter on the fault?

autocorrelation

Defined using the shape of the power spectrum

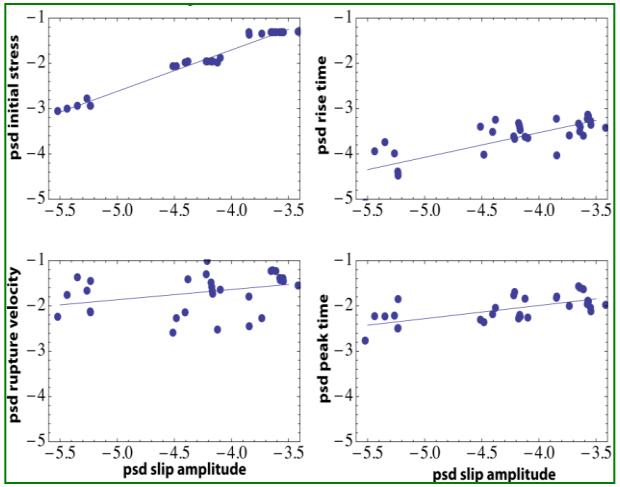

how are parameters related? correlations

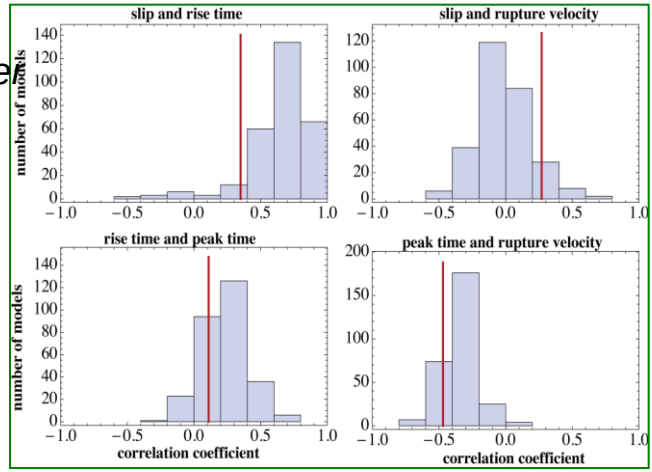

The values of rise time and peak time are adjusted such that the moment rate function fits a Brune spectrum for a specified corner frequency

Green Functions

Layered Earth model (1D)

1	α_1	β_1	ρ_1	h_1	Q_{P1}	Q_{s1}
2	α_2	β_2	ρ_2	h_2	Q_{P2}	Q_{s2}
3	α_3	β_3	ρ_3	h_3	Q_{P3}	Q_{s3}
	...					
n	α_n	β_n	ρ_n	h_n	Q_{Pn}	Q_{sn}

Frequency-wavenumber (FK) code
(Zhu and Rivera, 2001)

Is efficient for obtaining high-frequency synthetics, but they do not account for scattering effects that can reduce the influence of radiation patterns on high-frequency ground motions and increase the ground motion duration.

Ground motion: High frequencies

Randomized frequency dependent perturbation of strike, dip and rake (Pitarka et al, 2000)

$$\varphi_i = \begin{cases} \varphi_0 & f \le f_1 \\ \varphi_0 + (f - f_1) / f_2 - f_1)((2r_i - 1)\varphi_p, & f_1 < f < f_2 \\ \varphi_0 + (2 * r_i - 1) * \varphi_p & f_2 \le f \end{cases}$$

ϕ_0 is the given value of strike, dip or rake
ϕ_P is the maximum perturbation that can be added to ϕ_0 (e.g. 60, 15 and 30, respectively)
r_i is a random number uniformly distributed between 0 and 1
the subscript *i* denotes the index of point sources

with f1=1 Hz, f2=3.Hz

Randomness of the high frequencies is generated in the source description

Application: REAKT Project

WP7.10 – Objective: to carry out a feasibility study of an EEWS by investigating whether such a system could successfully be applied to sensitive objectives in the Eastern Caribbean region

VALIDATION OF THE METHOD

N.	Date	Time	Epicentral coordinates	Depth (km)	M_W	Strike Dip Rake (°)	Epicentral distance (km)
1	2000/10/04	14:37:45	11.15N 62.48W	110.4	6.1	277 42 141	170.2200

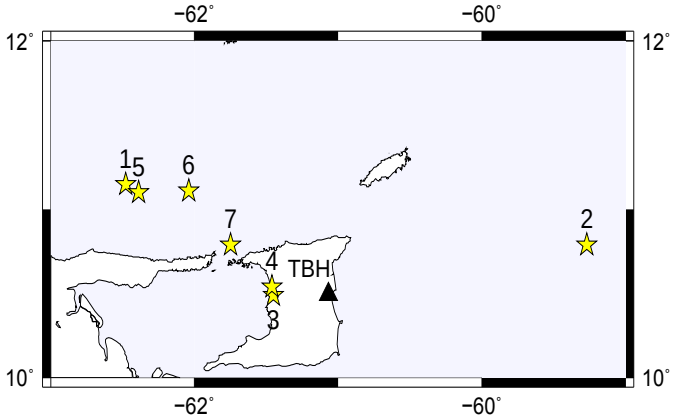

Low-frequency comparison (0.33-1 Hz)

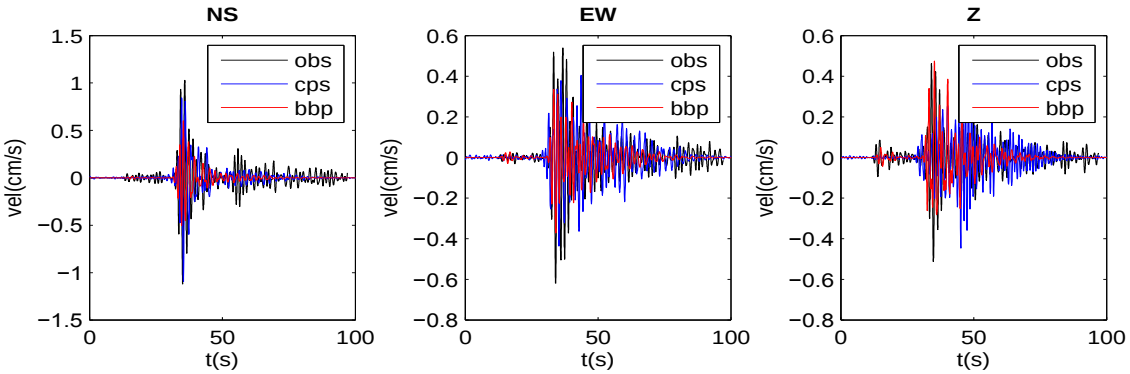

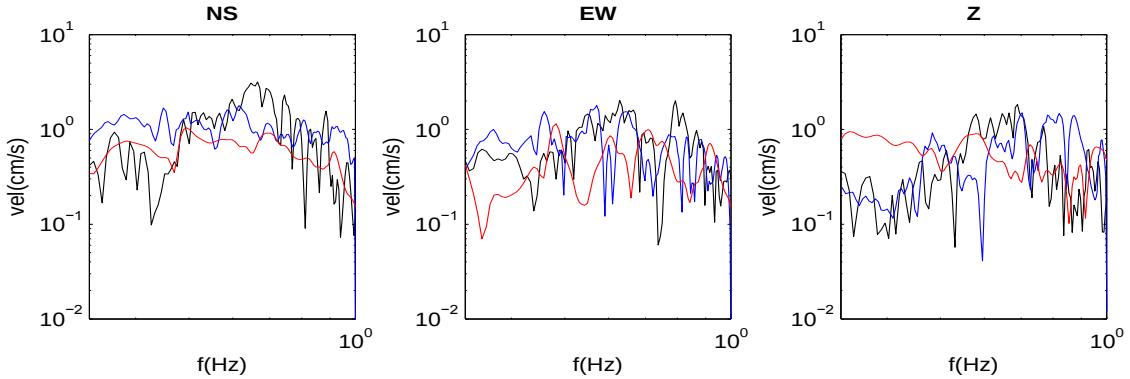

Recorded velocigrams
Computer Programs in Seismology (Herrmann, 2003)
Broadband (UCSB)

VALIDATION OF THE METHOD

N.	Date	Time	Epicentral coordinates	Depth (km)	M_W	Strike Dip Rake (°)	Epicentral distance (km)
1	2000/10/04	14:37:45	11.15N 62.48W	110.4	6.1	277 42 141	170.2200

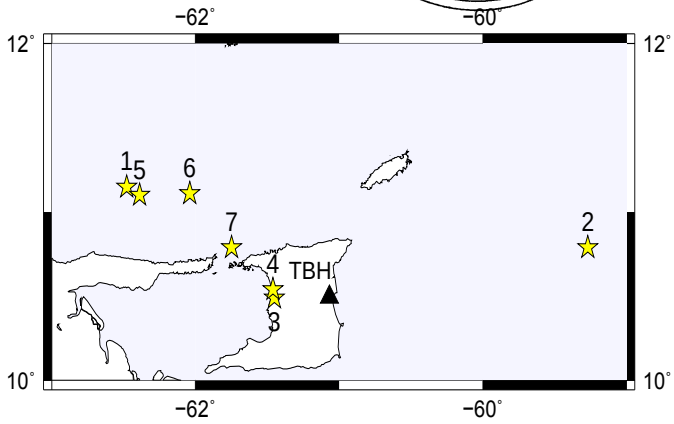

Recorded velocigrams
Broadband (UCSB)

Broadband comparison (0.33-10 Hz)

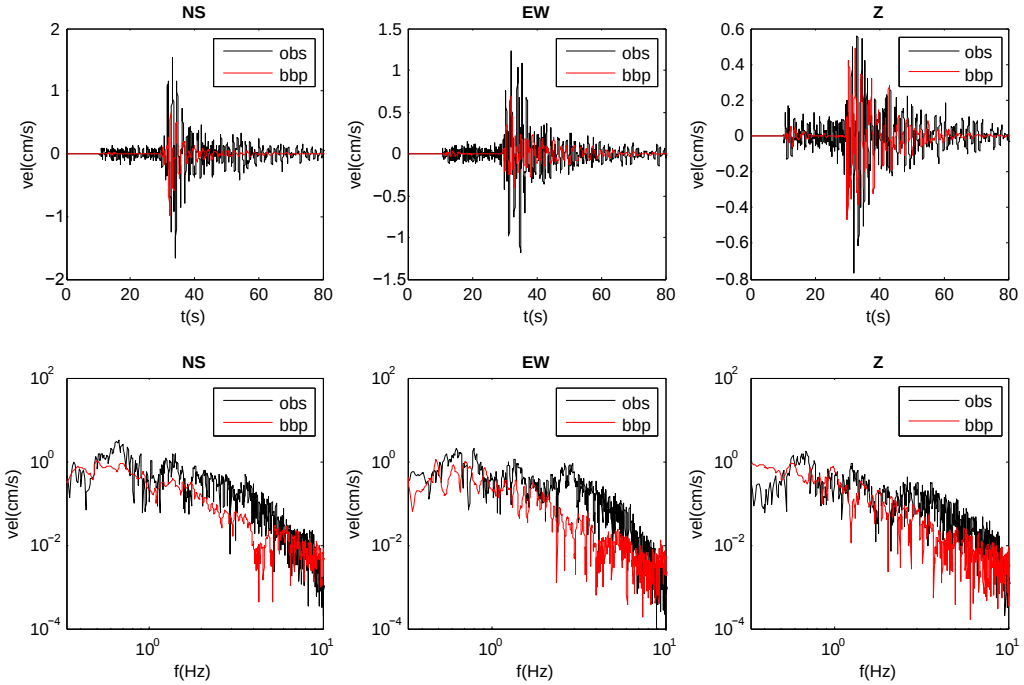

Even if the broadband modeling underestimates the frequency content at intermediate frequencies, modeling is able to reproduce quite well the arrival times, shape, duration and amplitudes of the waveforms
➔ ok for EEW

Mreal = 6.25, h=29 km

10 realizations of slip rate function distribution on the fault plane

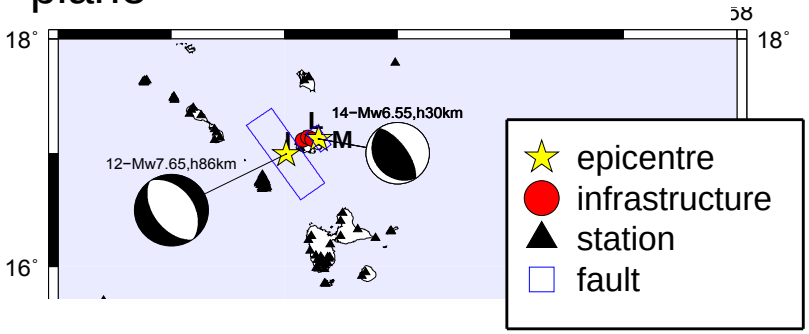

Zhao et al., 2006 GMPE

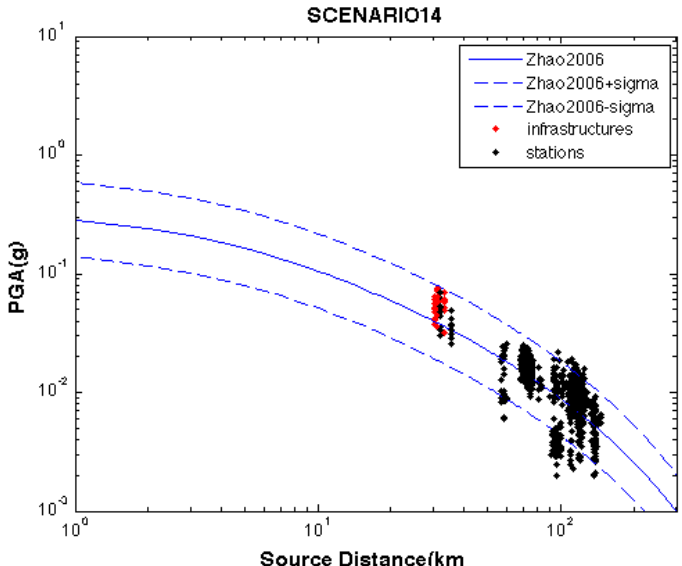

SEISCOMP3/VS PERFORMANCE (interface earthquake)

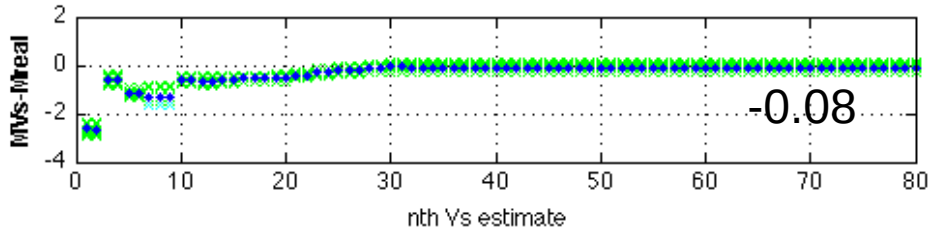

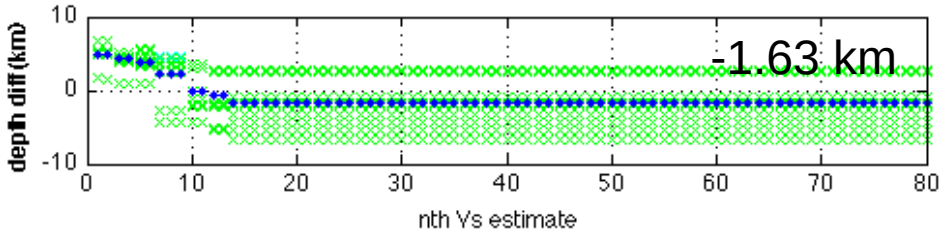

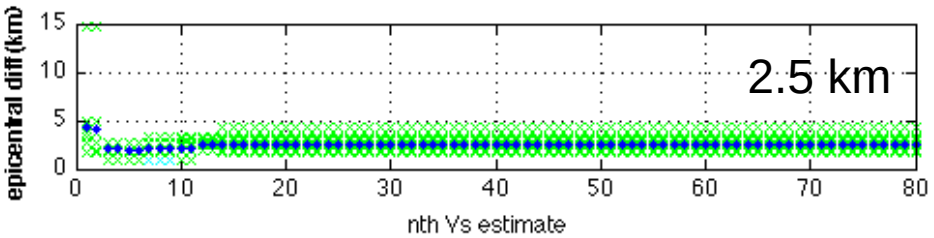

Cronoprogramma

TASK	DESCRIZIONE ATTIVITÀ	apr-14	mag-14	giu-14	lug-14	ago-14	set-14	ott-14	nov-14	dic-14	gen-15	feb-15	mar-15
A.1.1.	Validazione mediante il codice di calcolo in bassa freq. di Hisada-Bielak (2003)												
A.1.2.	Validazione mediante il codice di calcolo a banda larga sviluppato da UCSB e incluso nel BroadBand Platform												
A.2	Contributo alla creazione di una banca dati di accelerogrammi reali e sintetici pienamente caratterizzata in termini di meta-dati per gli effetti near-source												

Deliverables

1) Rapporto di sintesi sulle simulazioni compiute per il terremoto dell'Emilia del 20/05/2012, con valutazione della capacità predittiva e dei limiti dei codici di calcolo utilizzati.
2) Banca-dati di accelerogrammi (reali e sintetici) near –source compilata durante il precedente progetto ReLUIS.

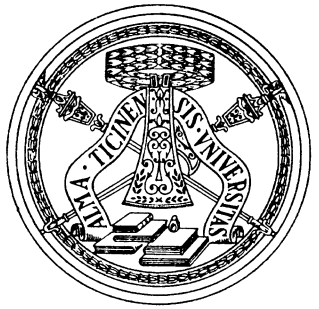

GRAZIE

Influence of focal mechanism on near-fault effects

The *radiation pattern of the shear dislocation* on a fault causes this large **pulse** to be **oriented in the direction perpendicular (or normal) to the fault**, causing the strike-normal ground motions to be larger than the strike-parallel ground motions at periods larger than 0.50s (Somerville, 2003).

M_w7.3 1992 Landers Earthquake (Lucern station)

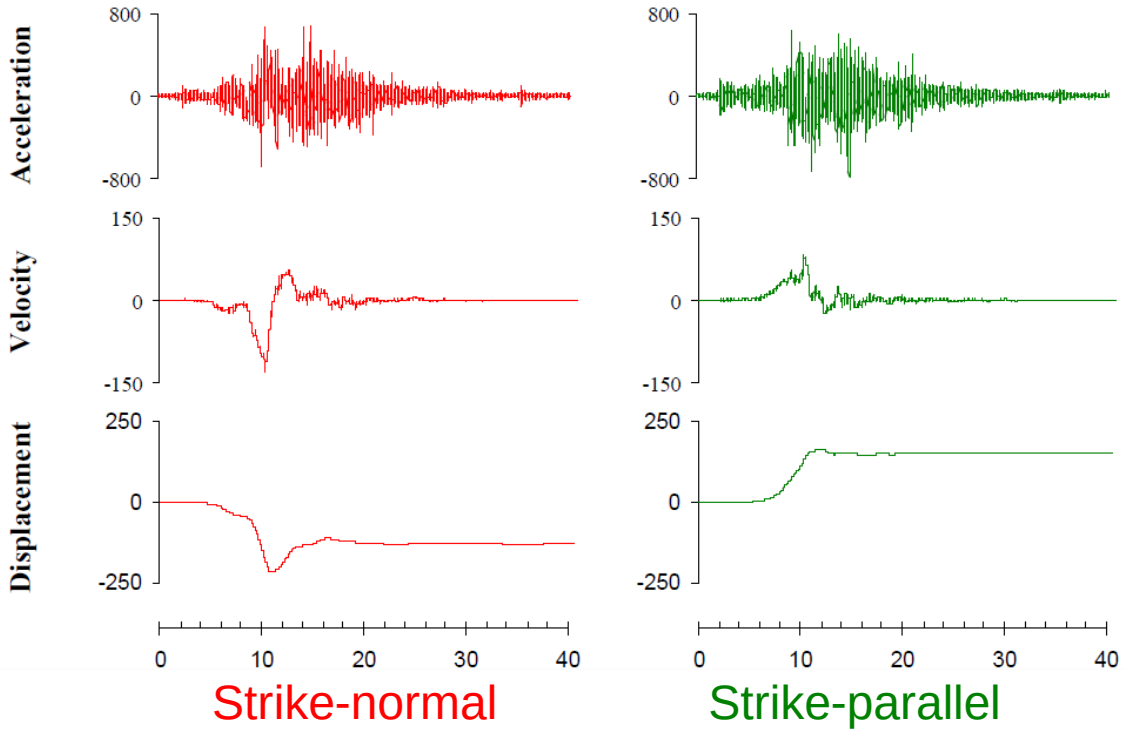

Strike-slip fault

Influence of focal mechanism on near-fault effects

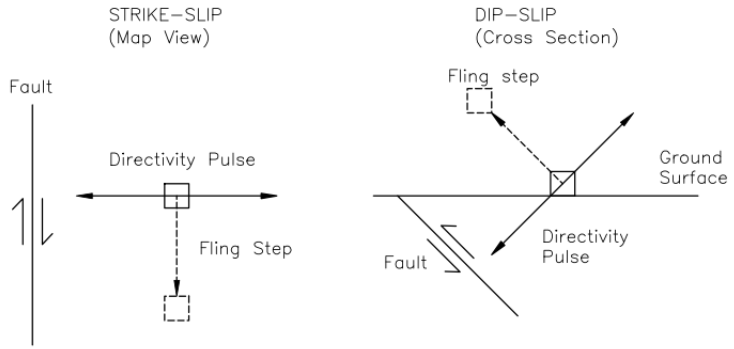

(from Somerville, 2005)

For dip-slip faults, the large rupture directivity pulse is oriented in the direction normal to the fault dip, and might be oriented in the strike-normal direction for large dip angles, or in the vertical component in case of low dip angles

Why synthetics dip-slip show impulse on SP instead than SN?

Pulse component

depend on rake/dip angles for dip-slip faults

larger

	Strike-parallel					Strike-normal				
Rake angle	Pulse Ind.	PGV (cm/s)	Late N, Y	Pulse N, Y	TP (s)	Pulse Ind.	PGV (cm/s)	Late N, Y	Pulse N, Y	TP (s)
0	1.0	189	N	Y	4.5	1.0	169	N	Y	5.3
15	1.0	178	N	Y	4.6	1.0	162	N	Y	5.1
30	1.0	157	N	Y	4.7	1.0	154	N	Y	4.9
45	1.0	151	N	Y	4.8	1.0	145	N	Y	4.6
60	1.0	149	N	Y	4.9	1.0	132	N	Y	4.5
75	1.0	141	N	Y	5.2	1.0	116	Y	N	3.9
90	1.0	129	N	Y	5.1	1.0	101	Y	N	3.3

Parametric analysis on rake (dip=40°)

	Strike-parallel					Strike-normal				
Dip angle	Pulse Ind.	PGV (cm/s)	Late N, Y	Pulse N, Y	Tp (s)	Pulse Ind.	PGV (cm/s)	Late N, Y	Pulse N, Y	Tp (s)
20	0.1	63	N	N	4.8	1.0	149	N	Y	5.9
30	1.0	99	N	Y	5.1	0.9	139	Y	N	4.3
35	1.0	107	N	Y	5.3	1.0	142	Y	N	3.7
40	1.0	129	N	Y	5.1	1.0	101	Y	N	3.3
45	1.0	152	N	Y	4.8	1.0	118	N	Y	3.1
50	1.0	167	N	Y	4.2	1.0	107	N	Y	2.9
60	1.0	179	N	Y	3.8	1.0	125	Y	N	2.4

Parametric analysis on dip (rake=90°)

Functional form: residuals

Step 1: A_f=a

Strong dependence on M_w and D

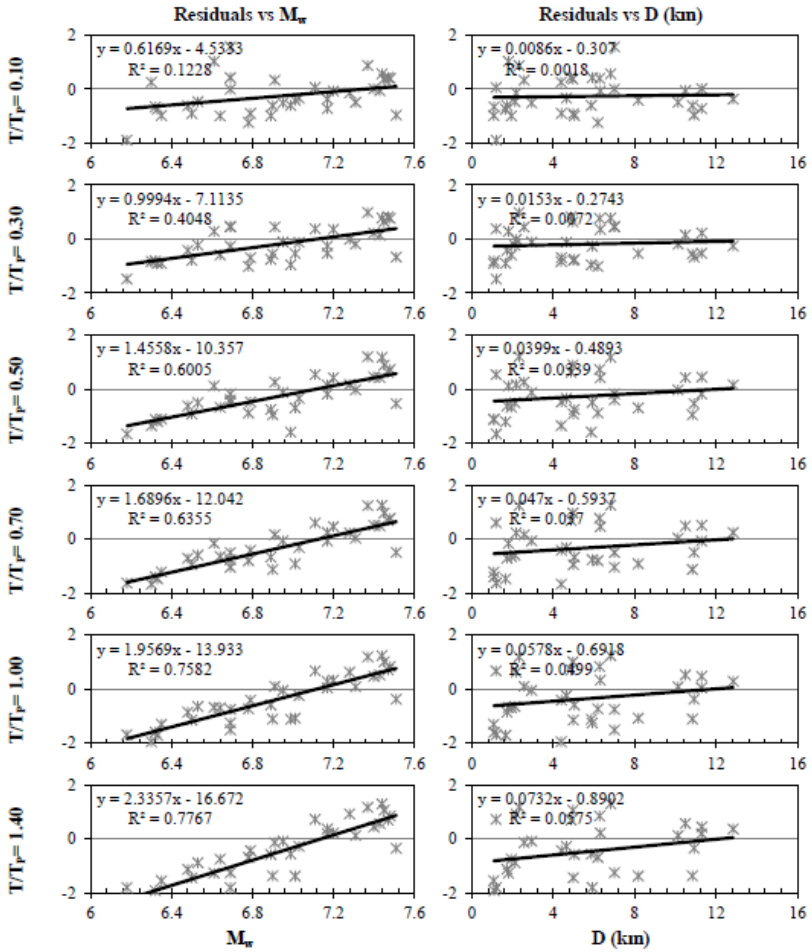

Step 3b: final step

Small dependence on M_w and D

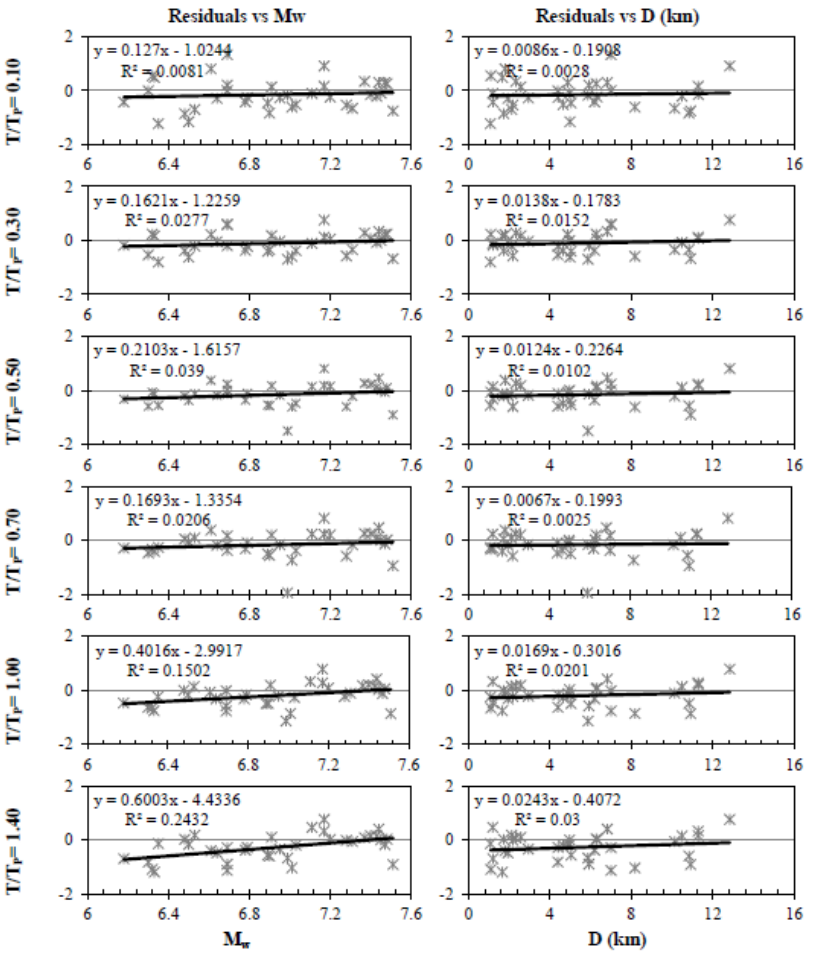

If soil types other than rock

Amplitudes and T_P have to be increased

EC8 for site class different than A

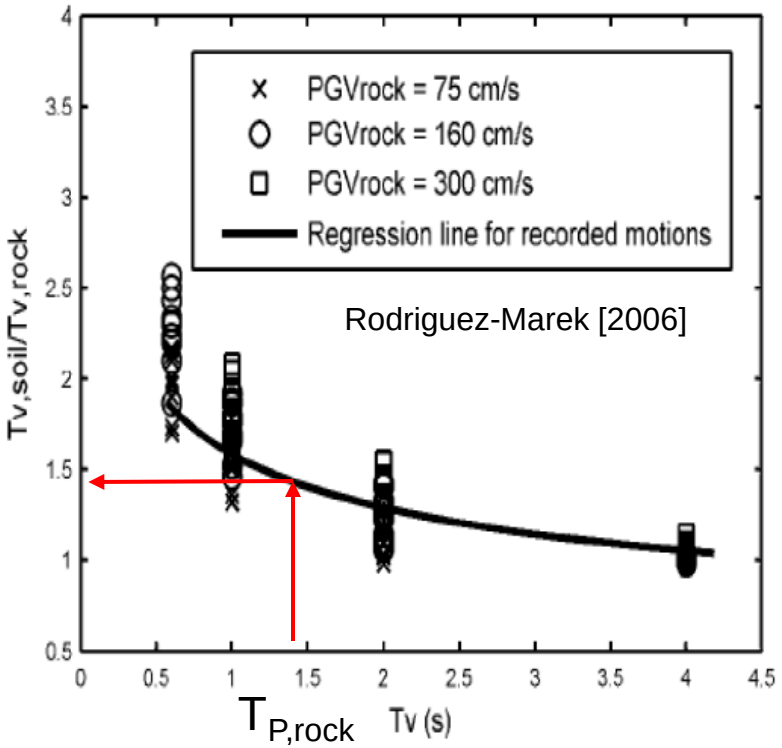

Comparison with NTC08

MEDIAN RESPONSE SPECTRA

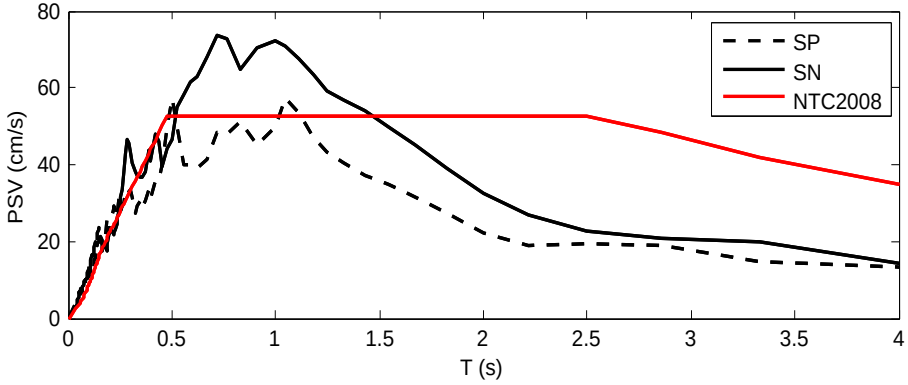

MEDIAN RESIDUAL RESPONSE SPECTRA